Androgen Modulation of MPP^+- Induced Dopamine release in the Corpus Striatum and Nucleus Accumbens of Male Rats

by

Lenka Fedorková

Submitted in Partial Fulfillment of the Requirements

for the Degree of

Master of Science

in the

Biological Sciences

Program

YOUNGSTOWN STATE UNIVERSITY

August, 1998

Androgen Modulation of MPP^+- Induced Dopamine Release in the Corpus Striatum and Nucleus Accumbens of Male Rats

by

Lenka Fedorková

I hereby release this thesis to the public. I understand this thesis will be housed at the Circulation Desk of the University library and will be available for public access. I also authorize the University or other individuals to make copies of this thesis as needed for scholarly research.

Signature:

Lenka Fedorková 8/7/98
Student Date

Approvals:

Robert E. Steiner 8/7/98
Thesis Advisor Date

Gary R. Walker 8/7/98
Committee Member Date

James R. Joseph 8/7/98
Committee Member Date

8/12/98
Dean of Graduate Studies Date

ABSTRACT

Androgen Modulation of MPP^+- Induced Dopamine Release in the Corpus Striatum and Nucleus Accumbens of Male Rats

Lenka Fedorková

Master of Science

Youngstown State University

Parkinson's disease is a progressive, neurodegenerative disorder of unknown cause found in elderly individuals. Its symptoms, such as uncontrolled tremors, difficulty in walking, and depression, are primarily due to low levels of the neurotransmitter, dopamine, which plays a major role in motor function. It has been demonstrated that specific cell death progressively occurs in the substantia nigra, a brain region rich in dopamine-containing neurons. This dopaminergic cell loss results in dopamine depletion in the neuron terminals found in the corpus striatum and nucleus accumbens. Furthermore, there seems to be evidence pointing to certain gender differences associated with Parkinson's disease, which suggests possible involvement of gonadal steroid hormones.

In order to better understand the processes involved, experiments have used the neurotoxin, MPP^+, which selectively destroys dopaminergic neurons. However, acute administration of MPP^+ stimulates dopamine release and prolongs its presence in the synaptic cleft by interfering with its re-uptake mechanism into the nerve terminals. The present study focused on the potential effects of castration in modulating the dynamics of acute MPP^+- induced dopamine release from the corpus striatum and nucleus accumbens in male rats. The technique of *in vivo* voltammetry was utilized for direct monitoring of evoked dopamine releases in these brain regions.

Results confirmed that specific dopamine release characteristics were suppressed following MPP^+ infusion in both the corpus striatum and nucleus accumbens when compared to potassium-stimulated responses. Results also demonstrated that MPP^+ was more effective in the nucleus accumbens than in the corpus striatum, suggesting a difference in sensitivity to this neurotoxin. Furthermore, castration altered the effects of MPP^+ in the nucleus accumbens suggesting that androgens may act in this brain region to influence the action of this neurotoxin in this area.

ACKNOWLEDGEMENTS

My utmost appreciation to:

--- Dr. Robert E. Leipheimer

--- Dr. Gary R. Walker

--- Dr. James R. Toepfer

--- Michael Arvin, Jr.

--- John Alcorn

--- Tonya Frost

--- Family and friends

Without whose guidance, help, and support I would never be able to complete this project. My sincere thanks and best wishes to you all !

TABLE OF CONTENTS

LIST OF FIGURES

CHAPTER I

INTRODUCTION :

Parkinson's Disease:

Parkinson's disease first described by James Parkinson in 1817 is an idiopathic neurodegenerative disorder of the dopaminergic nigrostriatal system occurring in elderly individuals. Certain factors that increase the likelihood of parkinsonism development include advanced age, coexisting brain damage, gender, genetic predisposition, and of course individual sensitivity to neuroleptic drugs (Pahwa and Koller, 1995). It is manifested by tremors, rigidity, impaired postural reflexes, bradykinesias or akinesias, and general difficulty in walking (Pahwa and Koller, 1995). These symptoms are due to cell loss in the nigrostriatal pathway of the extrapyramidal system (Session et al., 1994). It is typically associated with depression primarily in women with tardive dyskinesia (Bedard et al., 1977), a disorder characterized by bizarre, uncontrolled, and difficult movements of the facial musculature (Thompson, 1985). Other nonmotor symptoms include malfunctions of the autonomic nervous system, sensory disturbances such as loss of smell, and dementia (a possibly hereditary phenomenon). An important part of diagnosing parkinsonism involves demonstration of Lewy bodies in the tissue, which are round, eosinophilic inclusions contained within the degenerating neurons (Pahwa and Koller, 1995). There is believed

to be a long latent period before the onset of evident motor symptoms. Surprisingly, a reported 80% loss of striatal dopamine content can occur before Parkinson's disease develops (Pahwa and Koller, 1995). Parkinson's disease was the first disease of the central nervous system in which a defect in transmitter metabolism was shown to play a causal role. A breakthrough finding from Oleh Hornykiewicz's studies of postmortem human brains showed markedly low levels of dopamine, norepinephrine, and serotonin (Kandel et al., 1991). This was found in all brains from patients who had suffered from this disease. More importantly, of all these biogenic amines, dopamine concentrations were lowest, thus linking Parkinson's disease (PD) to a specific neurotransmitter deficiency (Kandel et al., 1991). In this disease (also called paralysis agitans), an assumed lesion is believed to occur between the pars compacta of the substantia nigra and corpus striatum and caudate nucleus (Thompson, 1985; Kandel et al., 1991). Further, abnormal outflow of transmitter occurs from globus pallidus to the ventral anterior and ventral lateral nuclei of the thalamus and then to the cortex, but it is the degeneration of the dopamine-containing neurons in the substantia nigra-basal ganglia system that causes PD (Thompson, 1985). There is likewise a degeneration of noradrenergic neurons in locus ceruleus and of serotonergic neurons in the raphe nuclei. Further, loss of dopaminergic extensions into areas of the limbic system like the nucleus accumbens, olfactory tubercle, and amygdala may be associated with some of the symptoms. For example, dopamine loss in nucleus accumbens may be partially responsible for akinesia (Kandel et al., 1991). In diseases of the basal ganglia such as this, abnormal movements usually result from a neuronal malfunction due to the destruction or dysfunction of some controlling (e.g. inhibitory) influences normally exerted on these neurons (Kandel et al., 1991). It is still uncertain

whether dopamine is excitatory or inhibitory to striatum neurons. If the input is excitatory, then loss of this excitatory input would account for the symptoms of bradykinesia and difficult initiation of movements (akinesia). If the input is inhibitory and lost, the positive signs of Parkinson's disease develop (Kandel et al., 1991).

Due to the fact that dopamine circuits are interrelated, treatment of Parkinson's disease has been complicated. Symptoms can be improved with a surgical intervention into the faulty outflow from globus pallidus into the thalamic nuclei thus alleviating symptoms of tremor and rigidity. However, the most disabling symptoms of bradykinesia do not subside and so this mode of treatment has largely been abandoned (Kandel et al., 1991). Administration of dopamine was ineffective since it cannot cross the blood-brain barrier. Briefly described, the brain permeability barrier is created by a continuous layer of vascular endothelial cells connected by tight junctions which present obstacles to chemicals on the basis of molecular size, charge, solubility, or specific carrier systems. The endothelial cells located within the cerebrum show a distinct absence of pinocytic vesicles and have characteristic, continuous intercellular zones of membrane preventing any leakage of chemicals in-between (Cooper et al., 1986). Levodopa (L-DOPA), the precursor of dopamine converted by the enzyme L-DOPA decarboxylase, on the other hand, is capable of crossing the blood-brain barrier and successfully stimulates dopaminergic neurons to produce more dopamine (Thompson, 1985). L-DOPA is presumed to be taken up into the cells, converted into dopamine, and then can be released affecting its target cells. This is accomplished by bypassing the initial rate-limiting conversion of tyrosine into L-DOPA by tyrosine hydroxylase (Kandel et al., 1991). Dopamine can also be generated by the action of L-DOPA decarboxylase

present almost everywhere in the brain and so even non-dopaminergic neurons contribute to increasing dopamine to levels sufficient for proper function of the remaining neurons. Unfortunately, L-DOPA therapy can produce dyskinesias due to the prolonged increase in dopamine levels. These symptoms can be reduced by antidopaminergic drugs (Bedard et al., 1977). Ironically, antipsychotic drugs such as neuroleptics used to reduce dopamine levels in schizophrenia patients lead toward the development of tardive dyskinesia over a long period of time. However, this is due to an excess of dopamine because lowered levels of the neurotransmitter cause the neurons to compensate and actually increase dopamine synthesis as well as express more receptors (Thompson, 1985). On the other hand, treatment with L-DOPA increases dopamine levels in Parkinson's patients, but at the same time may produce schizophrenia-like symptoms due to this effect. Also, dopaminergic agonists like L-DOPA, amphetamine, and apomorphine cause a stereotypic behavioral syndrome in rats and in other animals resulting in bizarre, repetitive acts like those seen in addicts or schizophrenics (Kandel et al., 1991). Nevertheless, L-DOPA administration has proven to be the most effective therapy for Parkinson's symptoms.

The true cause of Parkinson's disease is not known. In addition to the factors mentioned above, PD could be induced by unknown environmental agents or a number of neurotoxic compounds. There are environmental toxins, like paraquat and diquat that do not respond to levodopa therapy. Many of these environmental toxins interact with the dopaminergic system. Neuroleptics, for example, are dopaminergic blockers that lead to drug-induced PD that is more common in women and the elderly (Bedard et al., 1977). Furthermore, manganese found in mines or manganese-containing pesticides, ethanol withdrawal, DA depletors such as reserpine and tetra-

benazine, flunarizine and cinnarizine which block Ca^{++} entry, or the Ca^{++} - channel antagonist, diltiazem, are but a few of the many neurotoxins that can produce certain symptoms of parkinsonism (Pahwa and Koller, 1995). In contrast to these agents, only 1-methyl-4-phenyl-1,2,3,6-tetrahydro- pyridine (MPTP) produces true parkinsonism and responds positively to classical levodopa treatment. Therefore, it has been hypothesized that a similar compound may be the causant of PD (Pahwa and Koller, 1995).

Functional Neuroanatomy of the Basal Ganglia :

The basal ganglia are large masses of neurons embedded deep in the cerebrum. It is divided into three main subcortical nuclei: the caudate, putamen, and globus pallidus (i.e. paleostriatum). These are functionally interconnected with each other and with other subcortical nuclei, including the subthalamic nucleus and substantia nigra. The caudate and putamen nuclei are collectively termed the neostriatum or striatum, which together with the paleostriatum make up the corpus striatum (Kandel et al., 1991), an area rich in dopaminergic neuron terminals (Chiba et al., 1985). These five nuclei are involved in the integrated control of movement along with the cerebellum. The basal ganglia motor functions are mediated by the frontal cortex. Their main input comes from many areas of the neocortex (which suggests other functions in addition to motor control) and their output is directed through the thalamus to the prefrontal and premotor cortices (Kandel et al., 1991). The neostriatum containing the caudate and putamen nuclei, nucleus accumbens, and olfactory tubercle provide its major output to the substantia nigra and globus pallidus. These complex connections are via medium- sized neurons having densely spiny dendrites. The neostriatum receives major inputs from the cortex and thalamus. Its two subdivisions

include the limbic striatum (ventral) and the sensorimotor striatum (dorsal); the latter projecting into the substantia nigra (Smith and Bolam, 1990). The limbic system, composed of the nucleus accumbens, the nuclei of the stria terminalis, parts of the amygdala and hippocampus, and the lateral septal nuclei, originates in and receives input from the cell bodies of the ventral tegmental area located medial and superior to the substantia nigra. The areas of the limbic system are primarily involved in emotions, memory, and cognitive skills (Kandel et al., 1991).

A general striatal circuit can be described as that involving medium spiny neurons projecting from the striatum to parts of the thalamus, subcortical premotor areas, external segment of the pallidum to substantia nigra, and dopaminergic neurons looping back and receiving inputs from the cortex on its distal dendritic spines and from dopaminergic nerve terminals. Such connections have been demonstrated by retrograde study from the substantia nigra, whose targets are distal dendritic spines of the striatonigral neurons. The main function of these connections is believed to be for the dopaminergic input to interact with other inputs on the same spines (Smith and Bolam, 1990). Dendritic spines of the nucleus accumbens also receive a hippocampal input and a dopaminergic one. It is suspected, therefore, that the dopaminergic inputs into the dorsal and ventral striatal circuits are similar, thus explaining influences of the limbic system on the sensorimotor striatum. Different types of interactions exist between dopaminergic inputs and different parts of spiny dendrites. First, spines allow for a direct input from the cortex and a level of interaction at the distal and proximal end of the dendritic shaft. This suggests a clear modulatory role of released neurotransmitters, regulating the degree of excitability and responsiveness of a neuron to incoming signals. These striatal circuits may provide further

insight into the role of dopamine and its two classes of receptors, D_1 and D_2. D_2 receptors function on the striosomes (striatal patches) and D_1 receptors in the striatal matrix (Smith and Bolam, 1990). Due to this observation, it has been suggested that proper motor function requires simultaneous activation of both receptor types. More importantly, identification of the relationships between parts of the striatum may lead to a better understanding why certain motor functions are affected in Parkinson's disease and what their connection is to the areas involved with motivational and cognitive aspects of motor behavior (Smith and Bolam, 1990).

The substantia nigra is the largest nuclear mass of the mesencephalon and has two distinct zones: pars reticulata (ventral pale zone) and pars compacta (darkly-pigmented zone). It is unique because the cell bodies of the latter zone contain the pigment neuromelanin within its end-stage lysosomes and is responsible for the structure's dark appearance (Schwartz and Kandel, 1985; Thompson, 1985). The dark pigment is thought to be a polymer of dopamine or its metabolites. The neurons of pars compacta utilize dopamine as a neurotransmitter and its concentration directly reflects the degree of darkness in this region (Schwartz and Kandel, 1985). However, the function of this pigment is not known. Generally, substantia nigra (i.e. dark substance) is an area with many dopamine-rich neuron cell bodies (Javitch et al., 1985) which terminate in the striatum (specifically from pars compacta), nucleus accumbens, and locus ceruleus (Javitch et al., 1985; Schwartz and Kandel, 1985). Noteworthy is the fact that the latter two regions accumulate MPP^+ (a metabolite of MPTP) most readily since they possess the highest density of catecholamine uptake sites in the brain (Palacios and Wiederhold, 1984; Javitch et al., 1985). It should be added that the locus ceruleus is also a pigmented nucleus found in the brain stem containing primarily

norepinephrine – producing neurons (Schwartz and Kandel, 1985) and together with the substantia nigra undergo depigmentation and cell loss in parkinsonism (Pahwa and Koller, 1995). This is a very detrimental defect, considering that the pars compacta contains most of the dopaminergic neurons of the brain, housing about 80% of total dopamine content (Schwartz and Kandel, 1985; Thompson, 1985). Loss of dopamine in these sites may be chiefly responsible for the motor symptoms of Parkinson's disease.

Catecholamine Biosynthesis:

Catecholamines have a catechol nucleus consisting of a 3,4-dihydroxylated benzene ring. This group includes the neurotransmitters dopamine, norepinephrine, and epinephrine. Tyrosine is the common precursor molecule from which all of these are derived. The biosynthetic pathway involves five enzymes: tyrosine hydroxylase, aromatic amino acid decarboxylase, dopamine beta-hydroxylase, pteridine reductase, and phenylethanolamine- N-methyltransferase (PNMT). Tyrosine hydroxylase is the rate- limiting step for the synthesis of the catecholamines. It requires a reduced pteridine cofactor, which is then reoxidized by pteridine reductase, an enzyme not specific to neurons (Schwartz and Kandel, 1985). The first step in the reaction, therefore, involves the conversion of a tyrosine molecule reacting with an oxygen molecule to produce dopa by the action of tyrosine hydroxylase. Next, dopa is acted upon by aromatic amino acid decarboxylase and after releasing a molecule of carbon dioxide yields the production of dopamine. Dopamine beta-hydroxylase then converts dopamine, which again reacts with an oxygen molecule, to norepinephrine. The last step, catalyzed by phenylethanolamine-N-methyltransferase,

requires S-adenosylmethionine to provide a methyl group for the methylation of norepinephrine to epinephrine (Schwartz and Kandel, 1985; Lehninger et al., 1993).

Neurons code for specific enzymes which enables them to specialize in the synthesis of specific neurotransmitters (Thompson, 1985). For example, the dopaminergic neurons contain only the first two enzymes in the biochemical pathway (Thompson, 1985). Furthermore, norepinephrine and dopamine are synthesized at different rates mainly because there are higher levels of tyrosine hydroxylase found associated with the dopaminergic neurons (Cooper et al., 1986). Of all the areas in the brain that contain dopaminergic neurons, substantia nigra cell bodies have shown the highest tyrosine hydroxylase activity equal to 17.5+/- 2.7 nmoles of DOPA/mg protein/hr (Bacapoulos and Bhatnagar, 1977). Also, tyrosine hydroxylase can be inhibited reversibly by norepinephrine and dopamine, which bind the oxidized form of pteridine cofactor. When the enzyme is phosphorylated by a cyclic AMP-dependent protein kinase, its affinity for tyrosine and the pteridine cofactor is increased to overcome this end-product inhibition (Schwartz and Kandel, 1985). This affinity can be further increased by another protein phosphorylation, which requires Ca^{++} and calmodulin, especially for the hydroxylase originating from the striatum. Tyrosine hydroxylase that is bound to subcellular organelles is found to be more active than that located freely in the cytoplasm. Effects of this short-term regulation can be seen only over a period of days since all enzymes are synthesized in the cell body and require time to reach the terminals via axoplasmic flow (Schwartz and Kandel, 1985).

Dopamine Release, Signal Removal, and Metabolism :

When a nerve cell membrane depolarizes it generates an action potential, which is propagated down the axon. Upon reaching the axon terminal, voltage-gated Ca^{++} channels open, allowing extracellular Ca^{++} to diffuse into the terminal and exert its effects on dopamine storage vesicles (Battistin et al., 1996). These dopamine vesicles are closely associated with the plasma membrane and when stimulated, release their contents into the synaptic cleft by way of Ca^{++}-dependent exocytosis (Schwartz and Kandel, 1985; Battistin et al., 1996), figure 1. Dopamine molecules reaching the post-synaptic cell membrane can then bind reversibly to two different types of dopamine receptors and trigger a second messenger pathway. The receptors' modes of action are well-understood: the first, D_1 dopamine receptor activates adenylate cyclase which converts ATP to cyclic AMP and the other, D_2 dopamine receptor, also located post-synaptically is bound to a regulatory protein and inhibits the activity of adenylate cyclase. Of the two receptor types, D_2 possesses a much higher affinity for antipsychotic drugs and is acted upon more frequently by them (Schwartz and Kandel, 1985). Furthermore, located on the cell bodies and pre-synaptic terminals of nigrostriatal and mesolimbic dopaminergic neurons (Cooper et al., 1986) are inhibitory autoreceptors that are not linked to adenylate cyclase (Schwartz and Kandel, 1985). These autoreceptors regulate the release of dopamine from the storage vesicles, i.e. inhibit it when cytosolic dopamine concentration is too high (Cooper et al., 1986). The neurotransmitter then persists in the synapse until removed or degraded.

Figure 1. Dopaminergic nerve terminal. An action potential reaching the nerve terminal stimulates the storage vesicles to move toward the membrane and release dopamine by way of Ca^{++}-dependent exocytosis. This figure also illustrates MPP^{+}-induced dopamine secretion and the postulated mechanism of how MPP^{+} may enter through the mitochondrial outer membrane and interfere with the electron transport chain (insert).

PRESYNAPTIC DOPAMINERGIC NERVE TERMINAL

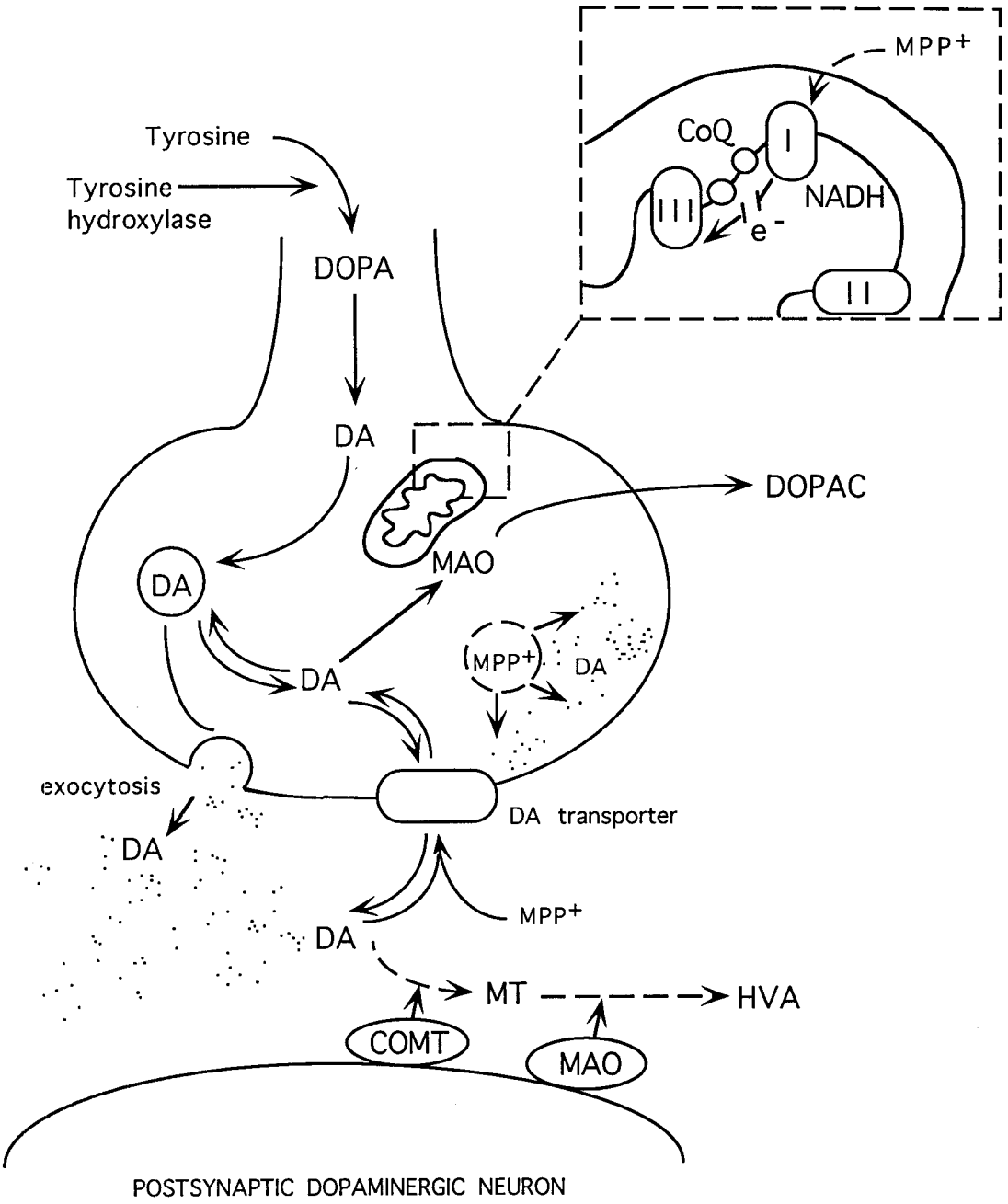

Neurons utilize several different means of terminating synaptic transmission. The neurotransmitters can be removed from the synaptic cleft by way of diffusion, enzymatic degradation, or by specific re-uptake mechanism. The re-uptake mechanisms are the most prevalent mode of signal clearance from the synapse. This is very important to allow expression of new, incoming signals. Specific, high- affinity sites at the pre-synaptic nerve terminal help to concentrate the neurotransmitter and bring it back into the terminal (Schwartz and Kandel, 1985). All biogenic amines, such as dopamine, are cleared from the synapse in this way. Once inside the terminal, dopamine can be degraded by specific intracellular enzymes such as the monoamine oxidase (MAO) (Schwartz and Kandel, 1985; Cooper et al., 1986). (The latter enzyme is found in many types of neurons, even in cells from liver and kidneys). COMT is located only on the post-synaptic cell and metabolizes dopamine into 3-methoxytyramine (MT). When dopamine is found freely in the nerve terminal it is susceptible to degradation by the cytoplasmic MAO associated with the outer membrane of the mitochondria. This MAO action produces the metabolite dihydroxy-phenylacetic acid (DOPAC) which is eliminated from the terminal. Smaller amounts of the MAO are located post-synaptically where it degrades dopamine left in the synaptic cleft and produces the metabolite homovanillic acid (HVA) (Cooper et al., 1985). Clearly, when dopamine is retrieved back into the terminal or is newly synthesized, it must be stored in vesicles in order to be protected from the enzymatic degradation. A vital role is played by the dopamine transporter, which pumps the neurotransmitter from the cytosol into the storage vesicles (Battistin et al., 1996) (Figure 1). When certain chemical blockers inhibit such a re-uptake mechanism, the effect of the neurotransmitter can be enhanced or prolonged at the post-synaptic cell.

Some substances act to displace dopamine by blocking its receptors, which can lead to a depletion of the amine (Schwartz and Kandel, 1985). In the central nervous system, dopamine is metabolized primarily into HVA and DOPAC and only small amounts of MT. During various studies, concentration determination of the HVA metabolite can help determine the level of activity in the dopaminergic neurons. For example, in Parkinson's disease where dopaminergic neurons are lost and dopamine levels are low, reduced amounts of HVA are observed in the cerebrospinal fluid. Stimulation of the nigrostriatal pathway, on the other hand, results in elevated HVA levels. Similarly, quantification of accumulated DOPAC in the striatum serves as a good indicator of dopaminergic nerve function (Cooper et al., 1986).

MPTP/ MPP^+ Neurotoxicity :

A neurotoxic contaminant of a street drug produced in the 1980's was isolated by researchers at Stanford University in 1983 (Cooper et al., 1986). The impurity formed during the chemical preparation of the narcotic meperidine which caused Parkinson-like symptoms was identified as 1-methyl-4-phenyl-1,2,3,6-tetrahydropyridine or MPTP (Javitch et al., 1985; Gerlach et al., 1991). MPTP was found to be specific in certain species and tissue types and exposure resulted in selective destruction of nigrostriatal dopaminergic neurons. MPTP, a cyclic tertiary allylamine (Chiba et al., 1984) now serves as a good experimental drug for the study of the mechanisms involved in idiopathic Parkinson's disease. Although, MPTP-induced neurotoxicity fails to produce Lewy bodies, a main neuropathological characteristic of PD in experimental animals and humans (Jellinger, 1989), most other known symptoms underlying idiopathic PD

correlate with MPTP-induced neurotoxicity. Initially, it was speculated that MPTP forms a reactive oxidation product which is neurotoxic (Cooper et al., 1986), but Chiba and colleagues demonstrated that MPTP exerts its toxic actions through its biotransformation intermediates (Chiba et al., 1984). MPTP itself has low chemical reactivity and is acted upon by central nervous system enzymes, like the ubiquitous monoamine oxidases (Chiba et al., 1985) or cytochrome P-450 mono-oxygenases, and is converted into more reactive compounds (Chiba et al., 1984). Indeed, the brain metabolizes MPTP into 1-methyl-4-phenyl-2,3-dihydropyridium cation ($MPDP^+$) and then into 1-methyl-4-phenylpyridine (MPP^+). This reaction is carried out by MAO-A and MAO-B enzymes found in the dopaminergic neurons (Gerlach et al., 1991). Through investigations of monoamine oxidase turnover rates, the B form was found to be more active and MPTP bound to it most readily. The density of MPTP binding sites on MAO-B in the substantia nigra and caudate nucleus of humans is more concentrated than in rats (Javitch et al., 1984). MPTP is, therefore, less toxic in rodents (Chiueh et al., 1984; Javitch et al., 1984). Interestingly, when a decrease in number of dopamine neurons occurs, no change in the number of MPP^+ binding sites is observed (Javitch et al., 1985). Administration of selective MAO-B blockers, such as L-deprenyl and pargyline, results in protection against MPTP neurotoxicity in mice and monkeys because these specific blockers inhibit conversion of MPTP to MPP^+ (Javitch et al., 1985), whereas, blockage of MAO-A does not (Chiba et al., 1984; Gerlach et al., 1991). However, it has been suggested that the conversion of MPTP to $MPDP^+$ does not occur inside the dopaminergic neurons, rather it is carried out by astrocytes (Ransom et al., 1987). It appears that astrocytes surrounding the dopaminergic neurons contain primarily MAO-B and are chiefly responsible for the

biotransformation of MPTP to $MPDP^+$ and then to MPP^+ (Gerlach et al., 1991). The MAO-B found in astrocytes is not present on catecholaminergic neurons (Chiba et al., 1985). The biotransformation of MPTP first involves a two-electron oxidation to yield the dihydropyridinium ion and then a four-electron oxidation into the phenylpyridinium ion (Chiba et al., 1984; Chiba et al., 1985). Production of such intermediates by MAO-B, which are electrophilic and can react with nucleophilic properties of neuronal macromolecules, can ultimately result in the initiation of neurotoxicity of dopaminergic neurons of the neostriatum (Chiba et al., 1984). The metabolites, $MPDP^+$ and MPP^+, exit the astrocytes either by way of diffusion or by forcefully damaging the cell membrane (Javitch et al., 1985). Outside the cell, $MPDP^+$ can form MPTP and MPP^+ independently of the processes inside the astrocytes (Chiba et al., 1985). Furthermore, astrocytes that bind and oxidize MPTP to its neurotoxic agent, MPP^+, subside to its toxic effect and are destroyed (Ransom et al., 1987). An important fact to remember, however, is that MPTP can be metabolized by MAO-A as well, and therefore its conversion could be taking place inside the dopaminergic neurons which contain this monoamine oxidase (Chiba et al., 1985). There is still a controversy concerning which form of MPTP enters the dopaminergic neurons. There is a possibility that MPTP is converted to $MPDP^+$, enters the cell, and is finally oxidized into MPP^+, or it is MPP^+ alone that serves as the appropriate substrate for the dopamine uptake (Chiba et al., 1985). Nevertheless, it is generally accepted that the metabolite MPP^+ is the neurotoxic form of MPTP in the nigrostriatal system (Irwin and Langston, 1985). It has been shown to be taken up selectively by the DA uptake system in the rat neostriatal tissue nerve terminals (Irwin and Langston, 1985). Del Zompo et al., (1992) further demonstrated that MPP^+ binds intracellularly

with high affinity to dopamine storage vesicles in nigrostriatal dopaminergic terminals (Del Zompo et al., 1992). Also, MPTP was found to have an affinity for neuromelanin derived from dopamine, which mediates the oxidation from $MPDP^+$ to MPP^+ (Gerlach et al., 1991), thus partially explaining the selective accumulation of the neurotoxin in the substantia nigra and not in other brain areas lacking this type of melanin (Irwin and Langston, 1985). Other studies found similar specific binding of MPP+ to the neuromelanin of primates and MAO of mouse brains (D'Amato et al., 1986; Del Zompo et al., 1990).

Dopamine and other catecholamines are taken up into the monoaminergic synaptic vesicles by an ATP-dependent vesicular monoamine transporter system. It has been shown that MPP^+ uptake into these vesicles is likewise an active, ATP-dependent process since no accumulation occurred when the transporter was inhibited by reserpine or when no ATP was available (Scherman et al., 1988). Administration of a selective and very potent dopamine-uptake blocker mazindol likewise prevents an MPTP-induced toxicity on nigrostriatal neurons in rodents (Javitch et al., 1985). This suggests that MPP^+ competes with dopamine for uptake into the striatal synaptosomes (Chiba et al., 1985; Javitch et al., 1985; Gerlach et al., 1991) (Figure 1). MPP^+ uptake into synaptosomes is highest in corpus striatum and described as sodium-dependent after a noted susceptibility to the Na^+K^+ - ATPase inhibitor, ouabain (Chiba et al., 1985). Additionally, MPP^+ uptake seems saturable and temperature- dependent, with minimal rate occurring at 4°C (Javitch et al., 1985). *In vivo* investigation of uptake characteristics of MPP^+ and dopamine showed very similar kinetic results: MPP^+ K_m= 0.48 mM and V_{max}= 5.3 nmol/g of tissue/ min; DA K_m= 0.18 mM and V_{max}= 3.5 nmol/g of tissue/min (Chiba et al., 1985), thus supporting the idea that MPP^+

and DA compete for the same active uptake mechanism into the striatal synaptosomal vesicles by the DA transporter (Chiba et al., 1985; Javitch et al., 1985). Animals treated with MPTP showed distinct lesions in the pars compacta neurons of the substantia nigra upon histological assessment. Additionally, locus ceruleus and ventral tegmental area dopaminergic neurons also exhibited damage (Gerlach et al., 1985; Javitch et al., 1985). Steranka et al.(1983) observed a depletion of DA stores and lesions in the dopaminergic neurons of the striatum. It is known that primates exhibit parkinsonism symptoms following MPTP/MPP^+ treatment and that their brains retain the neurotoxin the longest of all experimental animal models (Chang and Ramirez, 1986). There is a certain species difference in the degree of MPTP-induced neurotoxicity as primates and humans show specific patterns of cell death in nigrostriatal pathway that are less prominent in rodents (Javitch et al., 1985). Neurotoxicity by MPTP administration involves the following neurochemical alterations in the nigrostriatal pathway: DA concentrations are reduced, the metabolites DOPAC and HVA are also reduced in quantity, activity of tyrosine hydroxylase decreases, and DA receptor density on post-synaptic neurons decreases. Similar changes involving other neurotransmitters and in the nucleus accumbens have been reported (Gerlach et al., 1991).

Many biochemical reactions and functions of the dopaminergic neuron are affected by this neurotoxicity. The most evident biochemical change observed during cell death is the mitochondrial depletion of Ca^{++} and a subsequent decreased efflux of this ion across the plasma membrane, thus losing the transmembrane Ca^{++} gradient. The neurons become oversaturated with Ca^{++} and cell death ensues (Gerlach et al., 1991). Therefore, MPP^+ accumulation in the mitochondria of neurons changes the intracellular

mitochondrial Ca^{++} homeostasis. N-methyl-D-aspartate (NMDA) antagonists protect against this neurotoxicity by inhibiting excessive Ca^{++} inflow through receptor-operated channels (Gerlach et al., 1991).

Another intense area of study has been dealing with MPP^+ intervention of the NADH dehydrogenase function and inhibition of Complex I of the mitochondrial electron transport chain (Nicklas et al., 1985; Ramsay et al., 1986; Vyas et al., 1986; Mizuno et al., 1987). MPP^+ inhibits the NAD^+-linked substrates pyruvate/malate and glutamate/malate, but not succinate (Nicklas et al., 1985). This leads to the speculation that MPP^+ exerts its inhibition at a point between the high potential Fe-S cluster found in NADH dehydrogenase and the coenzyme ubiquinone (CoQ) located near the rotenone binding site (Gerlach et al., 1991), figure 1. Via this process, MPP^+ inhibits mitochondrial respiration and by consuming ATP stores (due to its energy-dependent nature) (Singer et al., 1987), renders the dopaminergic neurons unable to function properly (DiMonte et al., 1986). Both MPTP and MPP^+ cause ATP depletion in mouse brain synaptosomes as well (Scotcher et al., 1990), and so it seems that Complex I inhibition should be sufficient for dopaminergic neuron degeneration (Heikkila et al., 1985).

The actual dopaminergic nerve cell death is believed to be due to the generation of superoxides and cytotoxic free radicals when MPP^+ is reduced and reoxidized inside the neurons – this made possible by the MAO metabolism of MPTP (Poirier et al., 1985; Gerlach et al., 1991). Furthermore, free radical species can be generated by MPTP/MPP^+-induced autoxidation of DA (Poirier et al., 1985). If free radical generation is the mechanism of the evoked cell destruction, compounds such as free radical scavengers and antioxidants should protect against dopaminergic cell loss. However, results from other studies do not support this notion by

demonstrating a lack of dopaminergic neuron protection by metal chelators (Corsini et al., 1985; DiMonte et al., 1989) and ascorbic acid administration in the nigrostriatal areas (Gerlach et al., 1991). Thus arises the suggestion that $MPDP^+$, the active aldehyde intermediate, could act as the prime agent involved in the process of cell deterioration . Also, the substantia nigra has high concentrations of catalase and glutathione peroxidase when compared to other brain regions. Together with superoxide dismutase (SOD), these enzymes are involved in antioxidation reactions and provide natural protection for the tissue and so the reason for such susceptibility to MPTP remains a question. Part of the explanation could be the fact that dopamine and 6-hydroxydopamine undergo autoxidation which leads to the production of hydrogen peroxide and dopamine orthoquinone (Poirier et al., 1985). Superoxide mediates this autoxidation that can also be propelled by divalent metals, like manganese and iron found in abundance in substantia nigra. *In vitro*, MPTP potentiates dopamine autoxidation and *in vivo* it involves superoxide ($O_2^{\cdot}$), hydroxide ($OH^{\cdot}$), hydrogen peroxide, and maybe some transition metals when MPTP is being converted by MAO. From a number of transition metals, cobalt, iron, and manganese enhance MPTP- induced potentiation of dopamine autoxidation (Poirier et al., 1985). In the central nervous system, MPTP has an affinity for neuromelanin and by way of free radical production and the presence of metals it promotes formation of the neuromelanin precursor, aminochrome. It is, therefore, speculated that cell death in Parkinson's disease is also due to MPTP inhibition of lipid peroxidation in the neuromelanin pathway (Poirier et al., 1985).

A superfusion study of rat corpus striatum showed important effects of MPTP and its neurotoxic specie MPP^+ on endogenous DA and DOPAC releases (Chang and Ramirez, 1986). Both MPTP and MPP^+ inhibit DOPAC

release although MPP^+ has a greater effect as can be expected. Additionally, MPP^+ potentiates K^+ -induced DOPAC release and MPTP pretreatment does not (Chang and Ramirez, 1986). MPTP and MPP^+ infusion results in a dramatically increased DA release and again MPP^+ pretreatment enhances the K^+ effect and doubles the DA release rate. Overall, MPP^+ has a much faster and more potent influence on DA and DOPAC releases and in the case of dopamine it is associated with a lag period before DA levels reach their maximum (Chang and Ramirez, 1986). An explanation for this finding may lie within the possibility that MPP^+ inhibits the DA uptake mechanism and MAO activity, initially responsible for the relatively slow rise time, and that the lag period may be due to an accumulation of DA in the synapse and, at the same time, a slow clearance rate from the synaptic cleft (Chang and Ramirez, 1986). It is thought that MPP^+ might involve a direct DA secretion from terminal vesicles as well because DA levels compared to DOPAC levels are much higher after a stimulation (Chang and Ramirez, 1986).

Steroid Hormone Effects on Dopaminergic Neurons :

In recent years, research has been investigating the role of steroid hormones in the central nervous system and, more specifically, the emphasis has been on gonadal steroid hormone action on the affected dopaminergic neuron circuits in Parkinson's disease.. Generally, it is believed that steroids may modulate nerve action by affecting both genomic or membrane receptor mechanism pathways (Schumacher, 1990). The classic mechanism of action for steroid hormones involves a passive diffusion of the hormone across the cellular membrane, binding with a specific intracellular cytoplasmic or nuclear receptors, which activates other intracellular effectors, and ultimately leads to gene expression. Steroids may also bind to mitochondrial

membranes where they can regulate ATP production and thus the energy metabolism of the cell (Ramirez et al., 1996). It is believed that steroids can also cross the membrane barrier by way of endocytosis and thus would require specific membrane receptors. At the extracellular level, steroids are suspected of modulating the excitability of membranes, which may lead to altered firing rates of certain neurons (Ramirez et al., 1996).

The male brain, exhibits a tonic pattern for the regulation of hormone secretion, whereas the female brain shows a cyclic regulation of hormone secretion. Both genders possess receptors for both androgens (classic male sex steroid hormone) and estrogens (classic female sex steroid hormone), but vary in the neurons' ability to concentrate specific steroid hormones. Steroid-sensitive cells are found mainly in the preoptic area of hypothalamus, amygdala, midbrain, and spinal cord. For example, estrogen receptors can be found within cell bodies in the preoptic area (Schwartz and Kandel, 1985). A recent study identified a specific protein in the membrane that had a high binding affinity for 17B-estradiol and further noted that testosterone in different chemical configuration (B-orientation of 17-OH group on the D ring of steroid nucleus), similar to the natural structure of estradiol, competed for the binding site in olfactory bulb fractions (Ramirez et al., 1996). This suggests the possibility that estrogen and testosterone may share similar binding sites in the cellular membranes of other brain regions (Yamada and Nishida, 1978). The notion that steroid hormones might modulate activities of neurons in the brain by binding to membrane receptors has come about due to numerous observations that these modulatory actions take effect very quickly. This disputes the slow, classical genomic mode of action which may take anywhere from hours to days (Schumacher, 1990). Steroids have been described to rapidly affect neuronal plasma membrane

electrical activity, changes in firing frequency, changes in neurotransmitter receptors, release mechanisms for neurotransmitters, or ion channel activities. The specific second messenger system activated upon steroid-membrane receptor complex binding has not been described, but the involvement of cyclic nucleotides seems feasible (Schumacher, 1990). The possible existence of steroid membrane receptors has been further supported by experiments in which protein synthesis inhibitors failed to prevent these steroid hormones from exerting their actions. In several experiments, steroid hormones such as progesterone, estradiol, or testosterone conjugated to bovine serum albumin, (BSA changes the liposolubility to a hydrophilic complex), have been observed to bind to specific sites in various regions of rat brain (male and/or female) (Ramirez et al., 1996) and induce dopamine release from striatal nerve terminals (Dluzen and Ramirez, 1989; Schumacher, 1990). An example of rapid steroid hormone action has been demonstrated by progesterone and estrogen in nigrostriatal tissue inducing the release of dopamine (Becker, 1990a,b). Other direct interactions between steroids and neurotransmitters are the reduction of serotonin type1 receptors by estradiol or the fast conversion of D_2 dopamine receptors in striatum from high to low affinity states (Le'vesque et al., 1988). However, results of these studies must be interpreted with caution as the optimal experimental dosages of the steroids used have not been established. Under physiological concentrations, steroids diffuse across the lipid bilayer, however, at high concentrations they may cause undesired alterations in the membrane structure, which could account for some of the reported rapid actions of steroids (Schumacher, 1990). Research has demonstrated that gonadal steroids are involved in modulation of neurotransmitter production and release. This includes the monoamine transmitters, like dopamine or

norepinephrine (Bitar et al., 1992). The steroids affect the level of tyrosine hydroxylase and subsequently the synthesis of catecholamines. Effects on monoamines have been studied in areas of hippocampus, brainstem, and striatum (Bitar et al., 1992). Estrogen, progesterone, and androgen receptors have been localized in hippocampus and brainstem (Blaustein, 1986; Handa et al., 1987). The actions of estrogen and testosterone in striatal tissue has been investigated in many experiments, however, results vary tremendously and further, thorough investigation is required. Nevertheless, much useful information has been obtained about the modulatory effects of these gonadal steroids. Administration of estradiol produces an increase in DA turnover in the striatum of ovariectomized female rats and in castrated male rats estrogen treatment results in enhanced stereotypic behaviors (due to increase in DA) and a higher concentration of DA receptors in the striatum (Hruska et al., 1980; Bitar et al., 1992). Following gonadectomy in male and female rats, levels of the dopamine metabolites DOPAC and HVA increased dramatically and suggested an increase in DA metabolism in the hypothalamus and striatum of both sexes and in the brainstem of male rats. On the other hand, when the subjects were treated with chronic levels of testosterone or estradiol, the increased DOPAC and HVA levels failed to be reduced (Bitar et al., 1992). In contrast, administration of testosterone reduced activity of dopaminergic neurons in the brainstem of orchidectomized rats and in striatum of ovariectomized rats. These findings strongly suggest different modulatory effects of testosterone and estrogen in males and females in distinct brain areas (Bitar et al., 1992). Further, the sexually dimorphic nature of nigrostriatal dopamine pathway can be deduced. The interpretation that testosterone fails to reduce DA metabolism in the striatum in the above experiments is contradicted by a study

demonstrating that it acts to increase the activity of tyrosine hydroxylase (Kizer et al., 1978).

In addition to estrogen increasing striatal DA releases, it also enhances DA turnover and decreases the density of DA receptors in ovariectomized female rats (Le'vesque et al., 1988). Additionally, estrogen- treated male rats responded with increased concentration of D_1 dopamine receptors in the striatum (Hruska et al., 1982; Hruska et al., 1986). Membranes of male and female striatum may contain different proteins, which would partially explain why estrogen induces different effects on DA parameters in male and female rats. Becker (1990 b) and colleagues demonstrated a direct influence of estrogen on endogenous DA stores in the striatum (Becker, 1990b). The manner in which estrogen modulates DA release is still being investigated. The number of estrogen genome-activating receptors in striatum was observed to be very low and judging from the time and duration of responses, involvement of other modes of action should be considered (Becker, 1990b). Steroids can bind specifically to extracellular receptors, immerse themselves in the lipid bilayer, modify ion channels, and although lipophilic are rigid structures that can modify arrangement, structure, or dynamics of proteins within the membrane (Alfsen, 1983). Evidence for steroid membrane receptors in striatum has been reported for progesterone (Dluzen and Ramirez, 1984), which rapidly increase striatal DA release.

Estrogen has been implicated in its parkinsonism- promoting properties. These are mainly linked to the development of chorea-like movement disorders and tardive dyskinesia, which result from higher-than-normal dopamine levels (McDermott et al., 1994). Additional case study investigations have demonstrated the antidopaminergic effects of estrogen.

Worsening of symptoms in pre-menopausal women occurred following estrogen administration, intended to increase dopamine levels, but alleviated some of the dyskinesias in both men and women (Session et al., 1994). However, because Parkinson's disease is an age-related disorder with an average onset at 60 years of age, a time when women are devoid of endogenous estrogen, it may be that the lack of estrogen serves as a protective mechanism (McDermott et al., 1994). Clearly, the way in which estrogen affects Parkinson's disease is not well-understood. A possible explanation for the worsening of symptoms could be that estrogen may act via progesterone, which can mediate its antidopaminergic actions through endorphins (Session et al., 1994). Recently, a strong body of evidence was generated from studies in mice. Results demonstrated that estrogen facilitates the release of dopamine from the nigrostriatal tissue and even suggests that it has a neuroprotective role against MPTP-induced neurotoxicity in this brain region (Dluzen et al., 1996a). Gonadectomy of female mice resulted in decreased DA levels and treatment with estrogen increased overall DA turnover in corpus striatum even in mice treated with the neurotoxin. In addition, DA receptor concentrations in the striatum were increased. As discussed previously, MPTP actively competes with the DA re-uptake mechanism and causes DA depletion in the corpus striatum (Javitch et al., 1985). Estrogen appears to modulate the effectiveness of MPTP in altering DA homeostasis in the striatum. In this regard, the combined effects of MPTP and estrogen, which decreases DA uptake, may account for the ultimate neuroprotective action of the hormone (Dluzen et al., 1996a). When estrogen blocks the dopamine transporter, a subsequent decrease in DOPAC release and intraneuronal DA concentration and an increased DA release would follow. In similar fashion estrogen would

decrease MPP^+ uptake and inhibit its neurotoxicity (Dluzen et al., 1996a). Furthermore, the fact that MPTP and MPP^+ are competitive inhibitors of MAO-A and B types, could also account for the decreased concentration of extracellular DOPAC.

Interestingly, there seems to be a predisposition of males to developing PD due to reported dopamine depletion in the striatum as a result of naturally increased DA release and decreased DA content in this tissue (Diamond et al., 1990; Dluzen et al., 1996b). Thus far, clear gender-related differences in the course of the disease development and progression have not been established. A very important difference in the rate of mortality in men versus women exists nevertheless. Although women have a generally higher life expectancy, once they develop the disease have a 98% greater mortality rate (Diamond et al., 1990). This can only be speculated to be due to the hormonal or life style differences between men and women. This putative sex-linked difference in Parkinson's disease does not account for the duration of the illness since time of onset, physical condition of patients, or the age at which the disease is first diagnosed (Diamond et al., 1990).

A majority of studies have concentrated on the role of estrogen in modulating nigrostriatal dopaminergic activity or its interactions with MPTP/MPP^+-induced neurotoxicity (Becker, 1990a; Becker, 1990b; McDermott et al., 1994; Session et al., 1994; Dluzen et al., 1996a). However, reports that testosterone produces changes in this dopaminergic system have led to further considerations into its potential modulatory role in MPTP/MPP^+- induced neurotoxicity. Thus far, results concerning testosterone's effects on dopaminergic parameters have been contradictory. Castration of adult male rats leads to lower DA concentrations in superfused substantia nigra sections and decreases in DA and DOPAC levels in nucleus

accumbens (Mitchell and Stewart, 1989). Most studies, however, seem to agree on the antidopaminergic characteristics of testosterone (Engel et al., 1979; Dluzen et al., 1994; Dluzen et al., 1996b). This view can be justified by the clinical finding that male schizophrenic patients suffering from symptoms due to high dopamine levels, have low plasma testosterone levels (Engel et al., 1979; Dluzen et al., 1994). Evidence shows that testosterone decreases dopamine metabolism as indicated by lowered DOPAC and HVA levels in the rat striatum (Bitar et al., 1992) and decreased overall DA neuron activity (Engel et al., 1979). Interestingly, castration induced an increase in tyrosine concentrations, which increased the substrate available for tyrosine hydroxylase, and a subsequent increase in DA production (Engel et al., 1979). Additionally, MPTP-treated mice exhibited a decrease in L-DOPA-stimulated DA release after administration of testosterone to superfused striatum (Dluzen et al., 1994). Clearly, the dopaminergic nigrostriatal system is responsive to modulation by testosterone, which is well in agreement with the view of its antidopaminergic action. In contrast to the large amount of work done with estrogen, relatively little investigation has been directed toward a more thorough exploration of testosterone's actions on dopaminergic function or its interactions with the plasma membrane of nigrostriatal dopaminergic neurons. The types of techniques employed in experiments with this hormone, namely *in vivo* superfusion studies, may account for the diversity and contradictions that exist in the results. Furthermore, considering the fact that testosterone is aromatized to estrogen in the central nervous system, experiments may require the use of dihydrotestosterone (DHT, a 5 alpha-reduced metabolite of testosterone), which cannot be aromatized. Therefore, understanding whether certain

results are due to testosterone or estrogen derived from testosterone (although short-lived) would give more credibility to some results.

CHAPTER 2

MATERIALS AND METHODS:

Animals:

Adult male Long-Evans rats aged between 6-9 months and weighing 400-600g were housed in plastic cages either individually or in groups of two or three under a reversed 12-hour light-dark cycle (dark 1000 a.m.-2200 p.m.). Water and rat chow (Pro Labs 3000) were available *ad libitum*. A total of thirty rats were allocated for this study, of which twenty two resulted in successful data collection. One half of the animals were bilaterally sham-castrated (intact controls) and the remainder were bilaterally castrated two to four weeks prior to the beginning of the study in order to remove the natural source of testosterone.

Before the operation, all surgical instruments were thoroughly washed, then sterilized in a hot glass bead sterilizer. Surgeries were carried out under anesthesia by ketamine (50 mg/kg, im) and xylazine (8 mg/kg, im). The surgical site was shaved and prepped with ethanol and a 1 cm-long midscrotal skin incision was made. This was followed by bilateral incisions through the tunica albuginea. Whole testes with attached epididymis were removed from the scrotal sac and local vasculature and vas deferens were tied off. Surgical cuts were sutured and inspected each day after the operation. Animals designated for the sham-castrated group underwent similar treatment with the exception of gonadectomy to ensure equal surgical treatment of all subjects. All handling of animals used in this

experiment comply with the guidelines established by the Animal Care and Use Committee at Youngstown State University.

Stereotaxic Surgery:

On the day of an experiment one rat was anesthetized with urethane (1.5 mg/kg, ip). The anesthetic dosages per body weight were calculated into three equal portions administered in 20 to 25-minute intervals. The formula for dosage calculation was as follows:

$$\frac{\text{Body weight in kg} \times 5}{3} = \text{x number of cc unit}$$

After the last injection period elapsed, the animal was inspected for cornea and paw withdrawal reflexes. Once the animal was deeply anesthetized, it was carefully placed into a stereotaxic apparatus (Kopf, Tujunga, CA) so that the head was stabilized by a mouth clamp and two ear bars. The rat rested on a heating pad in order to maintain body temperature at 37 °C. The temperature was monitored by a rectal thermometer. Next, the dorsal aspect of the rat's head was shaved and cleaned with an alcohol swab. A medial incision was made rostro-caudally through the scalp and the skin was retracted and held in place with hemostats. The skull surface was gently scraped in order to remove connective tissue and dried with cotton tip applicators. The crossing between the coronal and sagittal sutures was used to locate the bregma reference point and label it with a permanent ink marker. The bregma serves as a guide for location of specific brain regions according to specific coordinate measurements. For this experiment, the coordinates given in the stereotaxic atlas by Paxinos and Watson (1998) for

location of the corpus striatum were 1.0-2.5 mm mediolaterally, 1.0-2.5 mm anteroposteriorly, and 3.0-7.5 mm dorsoventrally. In order to expose the surface of the brain, two surgical windows 4 x 6 mm were drilled out on each side rostrally from bregma (Figure 2). Two additional holes were made in the parietal bone approximately 4 mm behind the windows. A small metal screw was placed in one hole and two reference electrodes were inserted into the brain through the other hole. The reference electrodes were cemented in place with dental acrylic (Lang Dental MFG, Co., Chicago, IL). Care was taken to avoid spilling the acrylic into the surgical windows. The brain surface was kept covered with a moist piece of gauze until the experiment. It should also be noted that the brain surface remains protected by the dura mater, which is removed just before the recording begins.

In Vivo Voltammetry:

This experiment utilized the technique of *in vivo* chronoamperometry, also referred to as *in vivo* electrochemistry, for the monitoring of monoamine neurotransmitters in brain tissue. This method is comparable to a miniaturized version of high performance liquid chromatography (HPLC), which much like *in vivo* voltammetry exploits the oxidative property of amines like dopamine. The voltammetric mode of detection differs from HPLC in that it possesses a higher level of resolution capable of recording individual oxidation potentials of particular substances of interest. In order to record the electroactive compounds successfully, the type of electrode employed and the type of voltammetric measurement used (i.e. the way in

Figure 2. Rat skull with bregma landmark.

This figure illustrates the dorsal view of the rat skull. The bregma is at the intersection of the coronal and sagittal sutures, which serves as the reference point for coordinate measurements.

(Adapted from: Laboratory Anatomy of the White Rat, by Chiasson, R. B. 5th Ed.,Wm. C. Brown Publishers, Dubuque, Iowa, 1988, pp.4.)

RAT SKULL – BREGMA

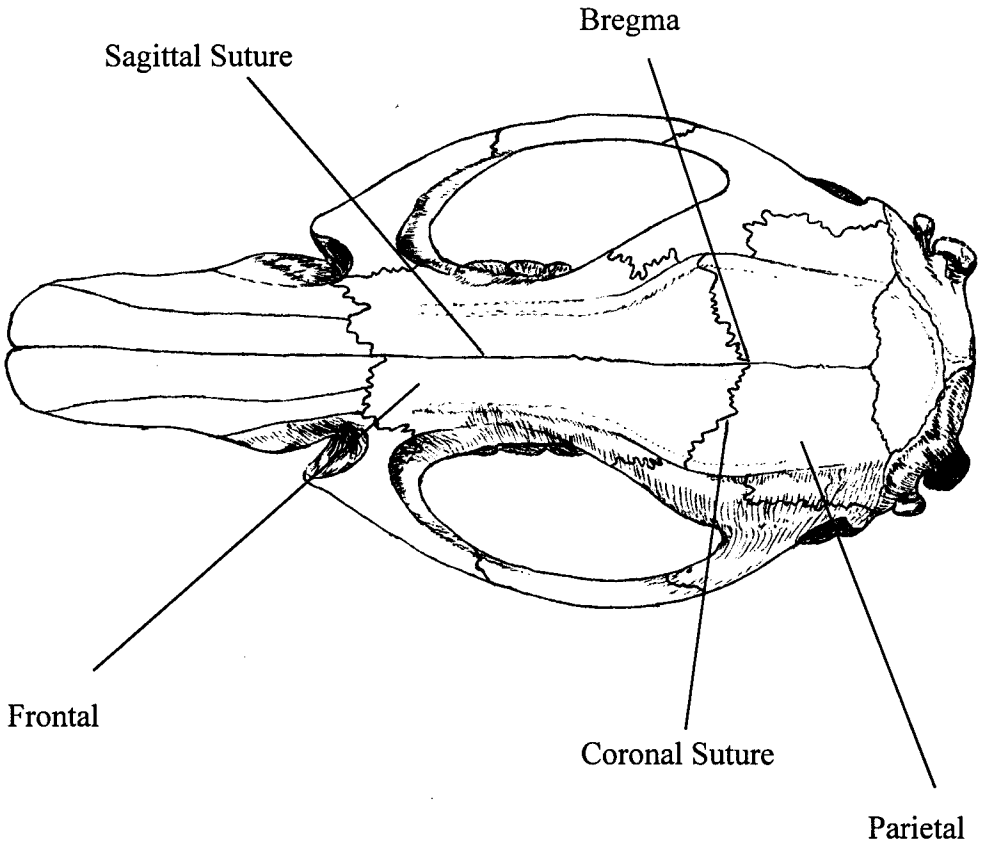

which the positive potential is applied) become crucial. The essential device used for monitoring compounds in the brain extracellular fluid (ECF) is a carbon-fiber electrode, in our instance, which plays the role of an oxidizing agent. It should be noted that *in vivo* voltammetric electrodes do not record concentrations of oxidizable species at the synaptic level. Instead, they measure the neurotransmitters or metabolites released into the extracellular space from synapses since most electrode diameters range from 1-1000 μm, while the size of a synapse is between 1-10 nm. A positive potential that is applied maximally to the electrode implanted in the neural tissue, as in chronoamperometry, causes dopamine to become oxidized. An oxidation current is thus generated by the liberated electrons travelling toward a reference electrode present in the vicinity of the carbon-based electrode. The working electrode records the oxidation and corresponding reduction currents occurring at its surface that are unique for each individual type of compound found in the ECF.

The extracellular fluid contains numerous indole- and catechol-based compounds, which can be easily oxidized. These substances can be distinguished from one another with relative ease as some undergo oxidation more readily than others due to a different level of potential applied. For example, dopamine oxidizes under a lower potential than its precursor, tyrosine, as DA possesses two hydroxyl groups, which give up their electrons more easily. Furthermore, catechols oxidize with greater ease than indols because hydroxyl groups lose electrons easier than NH-groups. Also, nervous tissue contains various compounds with similar oxidation potentials as the catecholamine of interest. Such is the case with ascorbic acid. It is present in corpus striatal tissue at sufficient levels to be detected at similar potential as dopamine. In order to be able to resolve between the two types

of signals produced, a working carbon-fiber electrode is treated and calibrated to highly select for a dopamine-like signal. This DA-like signal is referred to as dopamine in this thesis.

Working Electrode Assembly:

Single-carbon fiber working electrodes were hand-assembled in our laboratory from the following main components: carbon fiber (30 μm diameter; Textron Specialty Materials, Lowell, MA), glass capillaries (6" long, 1.0 mm o.d., 0.58 mm i.d.; A-M SYSTEMS, Inc., Cleveland, OH), epoxylite high temperature varnish (The EPOXYLITE Corp., Irvine, CA), lacquer-coated copper wire (28- AWG; Vector Electronic Co., North Hollywood, CA), and gold pin connectors (Newark Electronics, Newark, NJ). The overall process can be divided into four general steps spanning a period of several days.

First, using a horizontal micropipette puller (Flaming/Brown Micropipette Puller, SUTTER INSTRUMENT, CO., San Rafael, CA), glass capillaries were pulled so that a very finely tapered tip was produced. (The puller operated with a 2.5 mm x 2.5 mm box filament under the following settings: heat= 716, pull= 150, velocity= 70, time= 80.) Using the rough surface of a glass stopper, the tips were bumped back to create an opening of approximately 50-70 μm in size. The barrel portion was shortened to about 1 cm. The prepared tips were stored in a petri dish and covered. Next, carbon fibers were carefully sprayed down with a 95% ethanol in order to eliminate any possible particulate matter and static charge build-up. Once dry, the carbon fiber (1 cm) was inserted into the tip of the capillary through the barrel section so that it protruded through the tapered end. The fibers were

handled only with gloves or fine metal instruments to prevent contact with skin and other substances. A 36 gauge needle (Hamilton Co., Reno, NE) connected to the syringe was pushed inside toward the tip and a small drop of the manner were then placed into petri dishes and baked overnight in an oven at 110-120 °C. The following morning the electrode tips were carefully inspected under a microscope to see whether any glue may have leaked out and covered part of the carbon fiber. Should this be the case, such tips were discarded.

The second step in electrode building involved packing of the tips with the conductive graphite-epoxy paste and an insertion of a copper wire. Initially, a handful of the graphite-epoxy paste was scooped out of a container and placed on a piece of aluminum foil and left to thaw at room temperature until soft and malleable. (The paste should always be refrigerated and no older than six months as its components may start to disassociate.) Also, lacquer-coated copper wire was cut into 10-11 cm-long segments. About 5 mm of the lacquer paint was scraped off each end of the wire. The glass barrels were then held with hemostats and were pushed into the soft paste repeatedly until they started to fill with graphite-epoxy paste. An extra piece of wire was used to help move the paste inside toward the tip. Once the barrel section was completely filled with graphite-epoxy, the shaved end of a copper wire was cautiously inserted into the back end of the paste-filled electrode tip. These electrodes were then placed on petri dishes (about four to five per dish to prevent them from bumping into each other) and were baked in an oven set at 110-120 °C for approximately 10-12 hours (or overnight).

After curing, the junction of the copper wire and paste was sealed by applying a small amount of the epoxy glue. The electrodes were baked for

additional 10-12 hours at the same temperature to cure the back seal. When complete, each electrode was placed on a piece of paper and stabilized with a small piece of clay. While looking through a dissecting microscope with an ocular micrometer, the carbon fibers were cut with a scalpel to a length of 50 to 150 microns (please see figure 3). These single-fiber electrodes were stored in special containers in a dehumidified chamber. Before calibration, gold pin connectors were soldered at the other shaved end of the electrode wire.

Calibration:

The general purpose of calibration is to produce a working carbon-fiber electrode with adequate selectivity capable of recording oxidation currents generated by dopamine (DA) alone in the presence of ascorbic acid. Also, the electrode should be sensitive enough to detect physiological concentrations of DA expected (i.e. micromolar to nanomolar amounts). Before calibration, electrodes were coated with Nafion ™ (Aldrich Chemical Co. Inc., Milwaukee, WI). Nafion as a perfluorosulfonated derivative of Teflon ™, which is selectively permeable to cations and thus detects dopamine rather than its metabolites. More importantly, a highly-negatively charged Nafion coating on the surface of the carbon fiber strongly attracts the positively-charged molecules of dopamine and repels ascorbic acid and results in an increase in selectivity of the electrode for DA over ascorbic acid.

Electrodes were selected and dried for 5 minutes in an oven set at 160 degrees Celsius. Their tips were then carefully swirled for 2-3 seconds in a small Nafion-filled vial. The electrodes were then placed in petri dishes and

Figure 3. Single-fiber carbon electrode.

This drawing shows the carbon fiber electrode used for *in vivo* monitoring of dopamine releases.

SINGLE-FIBER CARBON ELECTRODE

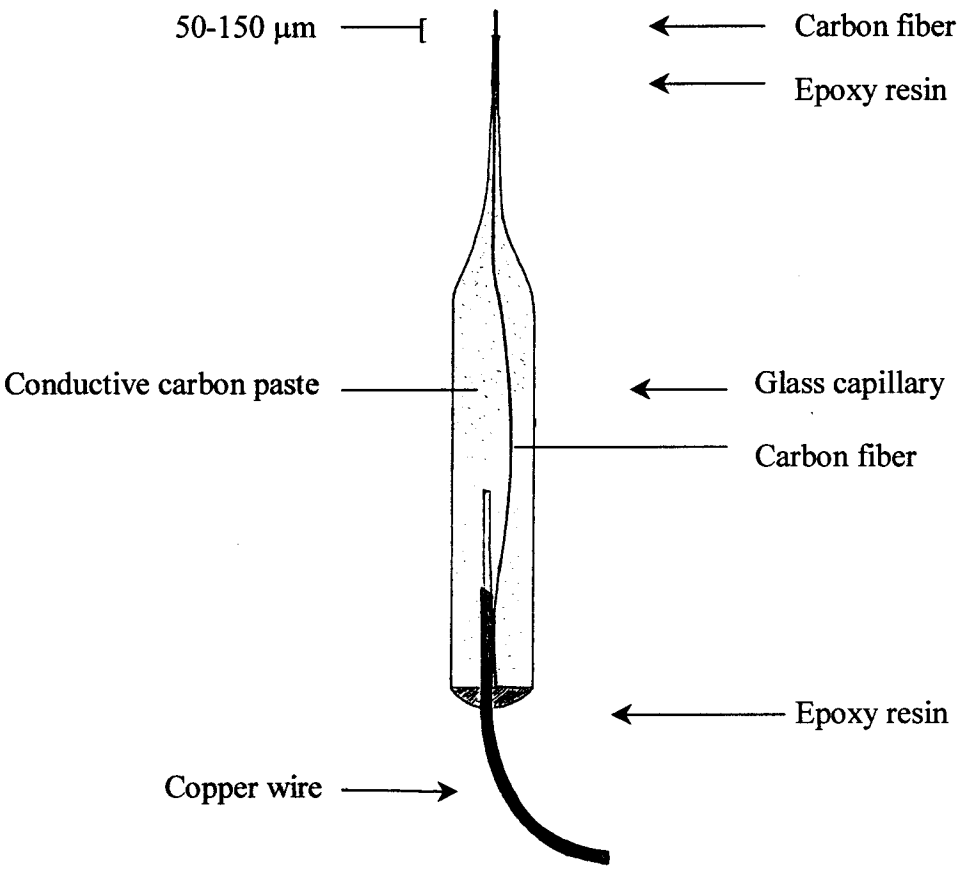

baked in an oven for 4 minutes. This step was repeated 4-5 times until a Nafion coating had developed around the carbon fiber. Next, solutions of 20 mM ascorbate (0.352 g ascorbic acid / 100 ml distilled water) and 2 mM dopamine (0.038 g DA / 100 ml 0.1 M perchloric acid) were mixed daily and weekly, respectively. A beaker containing 40 ml of 0.1 M phosphate buffered saline (PBS) solution was placed on a platform housing the headstage set at 100 V / μA. A silver-wire stable reference electrode was emersed into the beaker and connected into the appropriate port on the headstage. The tip of a Nafion-coated electrode was submerged into the beaker and connected to the headstage as well. The *in vitro* calibration was performed on a recording system, IVEC-10, consisting of the headstage and a signal amplifier connected to a Compudyne computer purchased from Medical Systems Corp. (Greenvale, NY). A calibration mode was selected from the Fast 12 program bar menu, which displayed a continuous record of the electrode currents and a window showing chronoamperometric oxidation and reduction waveforms plotted as functions of current (y-axis) over time in milliseconds (x-axis). Also displayed on the bottom of the screen was a table with slots for recording currents created during calibration, to be used for calculation of parameters describing the linear response of the probe.

The submerged electrode was initially allowed to stabilize for about 150-200 seconds. Gain amplifier settings were adjusted if necessary so that the template and actual electrode waveforms were closely correlated. First, 500 μl of ascorbic acid were added into the beaker and mixed. This event was marked and the average of ten preceding current values calculated was entered into the first slot of the table. Secondly, four to five additions of 40 μl of DA were made in the same manner, with each addition the total

concentration of DA being raised by 2 μM increments. The electrode should have responded to DA additions only. If the current values changed due to ascorbic acid, further Nafion coating and re-calibration in fresh buffer was needed to improve the electrode's selectivity. Once satisfactory calibration was achieved, the recorded data points were used by the computer to generate a regression curve (Figure 4). The regression curve is a graphical representation of the linear relationship between an oxidation/ reduction current and the micromolar concentrations of DA available for oxidation/ reduction. Through calibration, a series of other very important parameters are also determined. The oxidation slope is the main factor determining the sensitivity of the electrode to dopamine. For best results, this value should be higher than 100,000. The selectivity value based on the slope is given as a ratio of dopamine versus ascorbic acid; a number greater than 500 : 1 indicated an acceptable electrode. The signal to noise parameter, which should be less than 0.1000, determines how small a signal the electrode is capable of recording over a certain amount of noise in the recording system or the electrode itself. Also, the oxidation/ reduction ratio should range between 0.3-0.8 and the correlation coefficients should be as close to 1.0000 as possible. All these parameters were stored in the program and on hard copy which also included the headstage and amplifier gain settings.

Reference Electrodes:

Teflon-coated silver wire 0.008 inches in diameter (A-M SYSTEMS, Inc., Everett, WA) was cut into ca. 20 cm-long segments. A short section,

Figure 4. Regression curve.

This figure shows a graphical representation of the linear releation-ship between oxidation (top) / reduction (bottom) currents on y-axes and the micromolar concentrations of dopamine on the x-axis as obtained from the *in vitro* calibration.

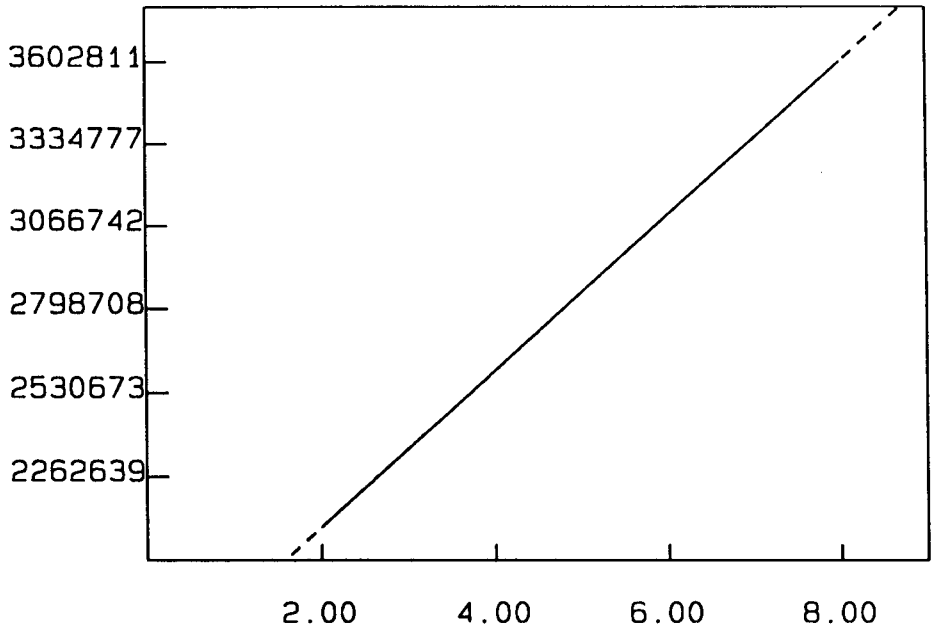

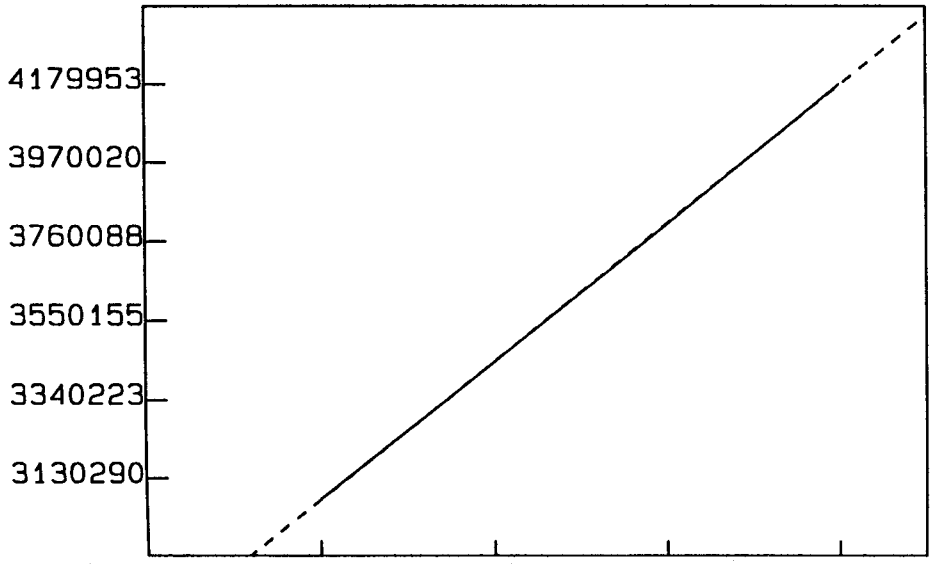

Mon Jan 12 21: 42: 31 1998

OXIDATION

SLOPE	250531.16
INTERCEPT	1599255.50
R^2	1.0000

ELECTRODE # 9

TRANSMITTER	Dopamine
RED/OX RATIO	0.74
SELECTIVITY	-1304849: 1
SIGNAL/NOISE	0.04279
FREQUENCY	5 Hz

REDUCTION

SLOPE	184178.80
INTERCEPT	2703964.00
R^2	1.0000

GAIN SETTING _____

FILTER SETTINGS _____

NAME _____

about 5-7 mm, of the Teflon insulation was shaved off one end and a gold pin connector (Newark Electronics, Newark, NJ) was soldered to it. Additionaly, 1 cm of the coating was removed from the other end, which was submerged into a beaker containing a supersaturated plating solution (40 g NaCl/ 100 ml 1M HCl) and a platinum cathode, the negative electrode of an electrolytic cell. In order to produce a silver/ silver chloride (Ag/ AgCl) reference electrode, a 10 Volt potential was applied to the plating bath for a duration of 20-25 minutes. In the end, a dark gray film formed around the shaved end of the wire. The reference electrode then cooled for additional 20 minutes. In the meantime, a second Ag/ AgCl reference electrode can be prepared because two reference electrodes are used during an experiment (one serving as a backup). Each plated wire was finally checked against a stable silver reference (Quanteon, Rocky Mountain Center for Sensory Technology, Denver, CO) submerged in a 3 M NaCl solution. In order to have established a stable reference, an Autograde Digital Multimeter 72-560 (Tenma Co.) digital display should register below 10 Volts. During the experiment, these electrodes implanted in the parietal cortex, one of which is connected to a headstage apparatus, provide the opposite pole for electrons to flow toward as a positive potential is applied to the working electrode, thus completing the electrical circuit.

Glass Micropipette Construction:

Glass capillary tubes (6 inches long, 1.0 mm o.d., 0.58 mm i.d.; A-M SYSTEMS, Inc., Everett, WA) were used to pull approximately 11 cm-long micropipettes on a horizontal puller (Flaming/ Brown Micropipette Puller,

Model P-80/PC, SUTTER INSTRUMENT CO., San Rafael, CA). The puller contained a 2.5 x 2.5 mm box filament (SUTTER INSTRUMENT CO., San Rafael, CA) and was operated under the following settings: heat = 716, pull = 150, velocity = 70, time = 80. The finely tapered tip placed on a microscope stage was carefully bumped back with the ground surface of a glass stopper. A 10-15 m tip opening was thus created. The glass micropipettes were stored in closed containers until later use during probe assembly.

Probe Assembly:

In order to be able to infuse chemicals, like MPP^+ and K^+ into the brain and measure the chemically-induced secretion, the probe apparatus was assembled. The calibrated electrode and a micropipette were aligned next to each other so that the glass tip and the carbon fiber protruding were perfectly even. While held together, the two were joined with sticky wax (Kerr ®, Romulus, MI) such that the distance between the tips lie within the range of 270-330 μm (Figure 5). This distance was visually confirmed under a light microscope with an ocular micrometer. This spacing is crucial to ensure that dopamine can be detected as it diffuses into the surrounding tissue. Next, with the use of a 31 gauge needle (World Precision Instruments, Inc., Sarasota, FL), the micropipette was back-filled with either an MPP^+ solution (0.00297 g/ 10 ml saline buffer; research Biochemicals International, Natick, MA) or a high K^+ solution (70 μM KCl, 79 μM NaCl, 2.5 μM CaCl; Sigma, Saint Luois, MO) depending on the experimental group investigated. Each solution was filtered through a 0.45 mm syringe

Figure 5. Recording assembly unit.

This drawing depicts the components and important dimensions of the probe assembly used during stereotaxic application of test substances and recording of DA signals generated. The glass pipette and the carbon fiber are joined with sticky wax (not shown) at the distance range indicated.

RECORDING ASSEMBLY UNIT

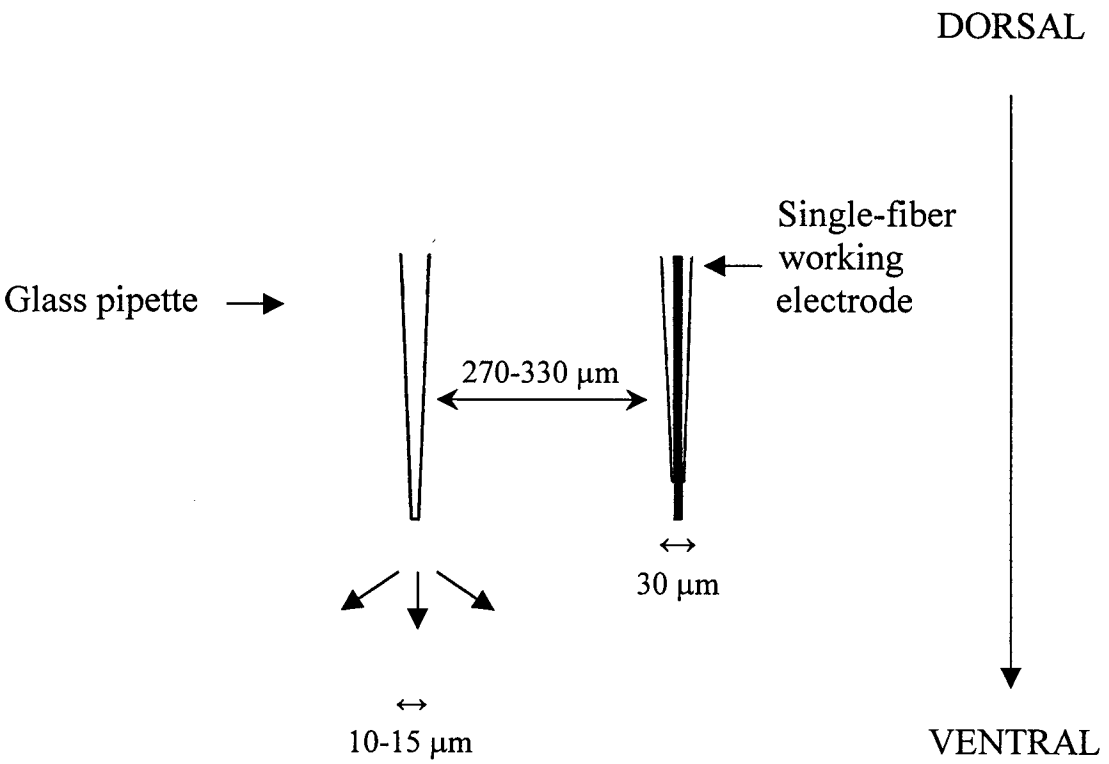

CORPUS STRIATAL TISSUE

filters (Micron Separation Inc., Westboro, MA) attached at the end of a 1 cc syringe.

Procedure:

Final preparation before data collection was made by attaching the working probe into the movable arm of the stereotaxic apparatus. The glass capillary tube filled with the test substance was connected to a nitrogen-operated picospritzer II (General Valve Corp., Fairfield, NJ) via rubber tubing. Dura mater was gently removed from the surface of the brain and the probe was positioned to the desired coordinates according to the stereotaxic atlas. Once a brain surface reading was obtained, the probe was slowly but steadily lowered 1.5 mm into the cortex. Calibration parameters stored in the computer's memory were recalled for the particular electrode used and the headstage settings were adjusted accordingly. Next, the acquisition mode was selected from the bar menu, which displayed the waveform for final verification of the electrode's status before proceeding to the data acquisition screen. A numbered scale on the y-axis represented the concentration of DA released and the x-axis, in seconds, served for the establishment of a baseline. Also displayed were the oxidation/ reduction waveforms for visual control of the electrode at all times, as well as the time remaining in a file and the time elapsed from a marked event. As the probe was first embedded in the brain tissue, it was allowed to equilibrate for 60-120 seconds (as indicated by a yellow baseline) prior to application of the electrical potential. During each pulse, the volume of the test substance was regulated by the duration and pressure settings on the picospritzer. Through the use of a dissecting microscope, volumes of the compound ejected were

determined from an ocular micrometer directed at the meniscus inside the capillary tube. (A single division on the micrometer was equivalent to 25 nl of substance). As a positive potential was delivered to the working electrode, the DA released in its proximity generated oxidation and reduction currents, which were in turn recorded by the working electrode. Subsequently, the electrical signal was represented on the monitor screen in form of a peak rising above the baseline. The amplitude of the signal directly correlated the amount of DA oxidized, thus allowing for real time recording of DA release dynamics at a sampling rate of 5 Hz. At the end of each event, the recording was stopped and individual release characteristics such as amplitude, rise time, T-50, and time course displayed were recorded on data sheets. Before another potential could be applied, the probe was moved ventrally through the corpus striatum and nucleus accumbens at 0.5 mm increments, while allowing for equilibration of the electrode between each pass as electroactive substances become quickly depleted in the area around the carbon fiber tip. Generally, injected volumes were between 175-250 nl for stimulation of DA secretion. On average, four or five passes were made in each surgical window at coordinates encompassing the location of the corpus striatum and nucleus accumbens (Figure 6).

Experimental Design:

In order to study the modulatory effects of testosterone on dopamine release dynamics evoked by direct potassium or MPP^+ infusion, animals were distributed into four experimental groups. The technique of in vivo voltammetry was utilized for the recording of induced dopamine releases from corpus striatum and nucleus accumbens of potassium-treated sham-

castrated (K^+/ Control), potassium-treated castrated (K^+/ CTX), MPP^+-treated sham-castrated (MPP^+/ Control), and MPP^+-treated castrated (MPP^+/ CTX) adult male rats. The following comparison groups were designed for the purpose of statistical analysis: 1) K^+/ Control vs K^+/CTX, 2) MPP^+/Control vs MPP^+/ CTX, and 3) K^+/ CTX vs MPP^+/ CTX.

Perfusion:

Following a successful experiment, the animal remained deeply anesthetized. It was carefully removed from the stereotaxic apparatus and placed on a surgical tray in a supine position with all four limbs secured. The entire procedure was performed over a sink. An incision was made transversely through the chest just above the diaphragm. While holding tissue scissors horizontally, to prevent puncturing of underlying organs, a second incision was made cranially about half an inch on either side of the sternum to expose the heart. The chest cavity was constantly rinsed with water to ensure a clear view of the heart and aorta. A large, 50-ml syringe was the filled with 0.9% physiological saline (Sigma Corp., Saint Louis, MO) and an 18 gauge needle attached at its end was inserted through the left ventricle into the aorta. At the same time, a small incision was made into the right atrium. As the contents of the syringe were emptied, a colorless liquid started to flow from the atrium indicating that the blood in the systemic circulation was being replaced. Further, another 50-ml syringe filled with 10% formalin (1:4 dilution, Fisher Scientific, Fair Lawn, NJ) was injected into the heart. The fixative reaching the organ tissues pushed out the

Figure 6. Cross-section of the rat brain.

This coronal section of the rat brain shows the location of the corpus striatum (CPU) and nucleus accumbens (NAc) .

(Adapted from: A Stereotaxic Atlas of the Rat Brain. 2nd Ed. New York; Plenum Press, 1979, by Pellegrino, L.J., Pellegrino, A.S., and Cushman, A.J.)

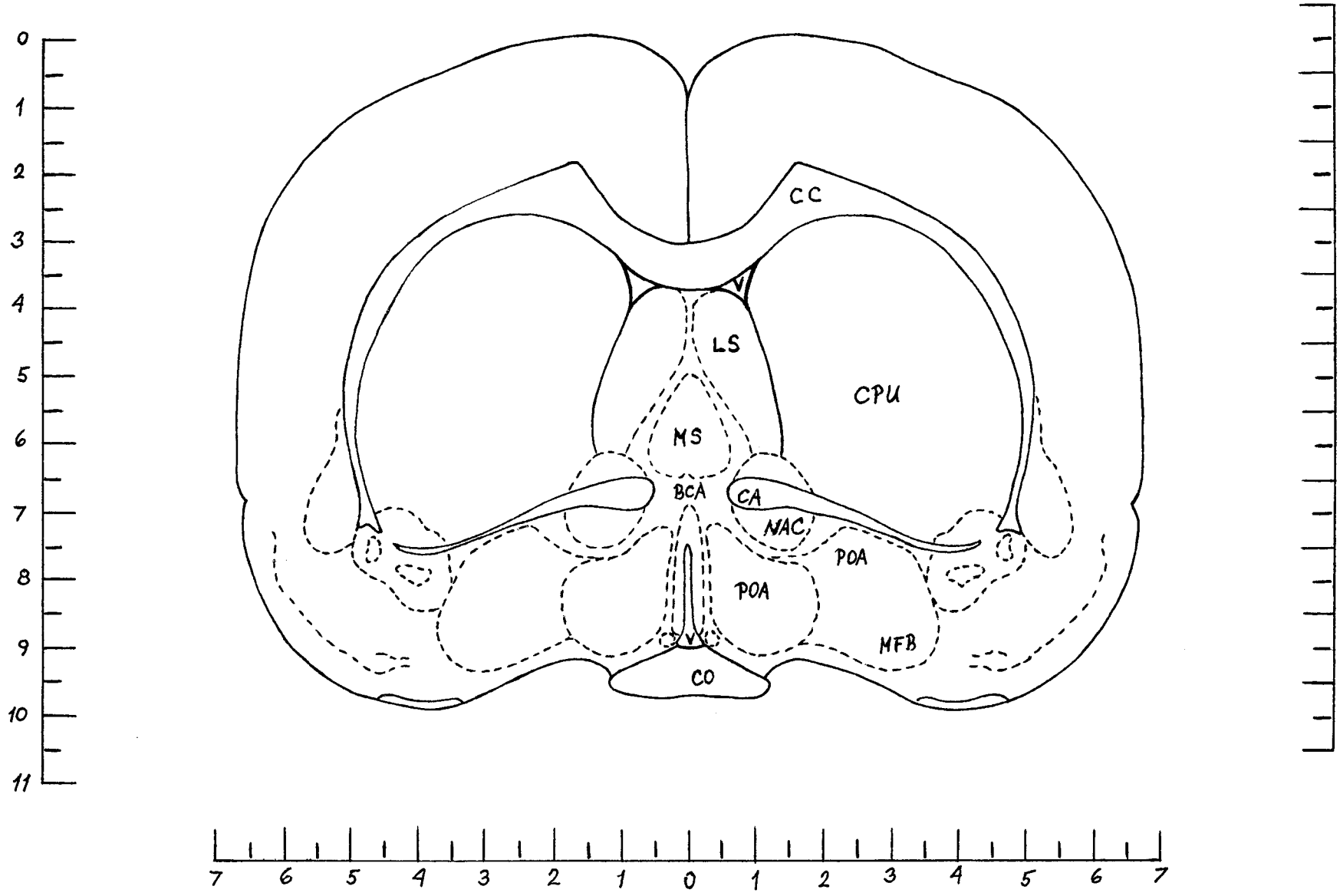
0
1
2
3
4
5
6
7
8
9
10
11
CC
LS
CPU
MS
BCA
CA
NAC
POA
POA
MFB
CO
7
6
5
4
3
2
1
0
1
2
3
4
5
6
7

remaining volume of blood and fixed the tissue.

Once the perfusion was completed, the rat's body was quickly decapitated using a small guillotine (Harvard Apparatus, Holliston, MA). With the help of rongeurs, bones of the cranium were chipped away until the whole brain could be removed, stored in a glass jar containing 10% formalin, and refrigerated.

Histology:

Fixed brains from all experimental groups were histologically evaluated for a confirmation of the electrode implantation path through the corpus striatum and nucleus accumbens. Whole brain was attached by freezing to the stage of a microtome (Cryo-histomat mK 2 model, Hacker Instruments, Inc., Fairfield, NJ). Coronal sections of the tissue were taken at a 30-micron thickness, while progressing rostro-caudally through the probed regions. The brain sections were placed in a sequence on numbered microscope slides coated with 20% bovine serum albumin (BSA) for better adherence. All slides were placed on a slide warmer and dried at 40 degrees Celsius. Once dry, prepared slides were submerged into glass coplin jars with 70% ethanol for 24 hours. The following protocol was utilized for the staining of the brain sections:

1) 20% EtOH – 3 min
2) distilled water – 3 min (3 x)
3) basic Fuchsin – 1.5 min
4) distilled water – rinse
5) distilled water – 3 min
6) acid formalin – 5 sec
7) distilled water - rinse
8) distilled water – 3 min

9) 70% EtOH – 3 min
10) 95% EtOH – 3 min
11) 100% EtOH – 3 min
12) 100% EtOH – 3 min
13) xylene – 5 min
14) xylene – 5 min
15) cover with permount and cover slip

Prepared slides were visually inspected in order to verify the placement of the working electrode under a light microscope.

Statistical Analysis:

Unpaired t-test (Sigma Stat 1.0, Jandell Scientific, Corte Madera, CA) was used to analyze specific parameters of dopamine release, such as amplitude, rise time, secretion rate, clearance rate, T-50, T-20-60, T-40-80, and time course of the release event for the comparison groups. The averaged values were graphically represented using a Sigma Plot 1.02 program (Jandell Scientific) and expressed as means of ± S.E.M. Differences between the groups having $p < 0.05$ were considered statistically significant.

CHAPTER 3

RESULTS:

Data from twenty-two male rats were analyzed for DA release characteristics in the corpus striatum (CPU) and nucleus accumbens (NAc) using the technique of *in vivo* voltammetry.

In the five potassium-treated sham-castrated males (K^+/Ctrl) ninety-nine DA releases were analyzed from the CPU and eleven from the NAc. Potassium treatment of the castrated animals (K^+/CTX) resulted in one hundred sixteen DA releases from the CPU and twenty from the NAc. One hundred forty-three and thirty-four DA releases were recorded in the CPU and NAc, respectively, from six MPP^+-treated sham-castrated (MPP^+/Ctrl) animals. Lastly, from the five MPP^+-treated castrates (MPP^+/CTX), one hundred one DA releases were recorded in the CPU and thirty-one DA releases in the NAc.

The IVEC-10 neurotransmitter analyzing program calculated a number of specific characteristics for each individual DA response. Examples of typical K^+ and MPP^+- induced DA releases are shown in figures 7 and 8, respectively. Figure 9 depicts a comparison between a typical K^+- induced DA release (top) and an MPP^+- induced DA release (bottom). From visual evaluation alone the two releases possess notably different characteristics as was expected due to the different modes of action of potassium and MPP^+. The differences between K^+ and MPP^+- stimulated DA releases were observed in all parameters analyzed and were evident in both the corpus striatum and nucleus accumbens regions. (Please refer to

figures 10-17 and 18-25 for comparison of individual parameters.) Overall, DA release was drastically reduced following MPP^+ administration thus resulting in decreased amplitudes. Also noted were decreased secretion rates and longer rise times. MPP^+- stimulated DA releases also had decreased clearance rates and substantially longer T-50, T-20-60, and T-40-80 decay times. On average, the total duration of K^+ or MPP^+ - stimulated DA releases described by the calculated time course values were quite similar.

DA release in K^+/Ctrl versus K^+/CTX in CPU and NAc:

Differences between DA releases in the CPU and NAc of K^+- treated intact (control) and castrated animals are represented in figures 10-17. Statistical evaluation revealed specific differences in DA release dynamics as a result of castration. Furthermore, variations in DA secretion were found between CPU and NAc. In these and all subsequent figures the following key is used to designate the comparison groups analyzed statistically: 1) K^+/Ctrl or MPP^+/Ctrl versus K^+/CTX or MPP^+/CTX in CPU; 2) K^+/Ctrl or MPP^+/Ctrl versus K^+/CTX or MPP^+/CTX in NAc; 3) K^+/Ctrl or MPP^+/Ctrl in CPU versus K^+/Ctrl or MPP^+/Ctrl in NAc; and 4) K^+/CTX or MPP^+/CTX in CPU versus K^+/CTX or MPP^+/CTX in NAc. No statistical differences in amplitude were observed between the intact and castrated animals in either CPU or NAc. However, NAc showed almost 70% smaller DA concentrations released than in CPU in both intact and castrated rats (Figure 10: 2.72± 0.213, 2.77± 0.221 versus 1.59± 0.519, 1.66± 0.553 μM). Figure 11 illustrates DA rise times for intact and castrated groups, which reached similar values within each brain region. The rise time in the K^+/CTX was significantly faster in the NAc ($p = 0.0188$) than in the CPU (14.3±1.70

versus 20.6±1.07 sec). The secretion rate shown in figure 12 was slightly, but not significantly, increased in both treatment groups in the CPU (142.6±11.3 and 141.3±10.6 nM/sec) when compared to secretion rates obtained from the NAc (76.1±20.4 and 107.9±28.9 nM/sec. The T-50 of DA release for both brain regions is represented in figure 13. Differences in the T-50 parameter were not observed between the intact and castrated animals in the CPU, but a significantly decreased T-50 was found in the NAc of K^+-treated castrated males (25.5±3.27 sec) when compared to the intact animals (36.7±3.95 sec). This statistical difference ($p = 0.0427$) represents a 44% faster DA decay time in the NAc of castrated subjects. Also, the T-50 of castrated animals was significantly longer in the CPU (39.1±2.10 sec) than in the NAc (25.5±3.27 sec), $p = 0.0107$. The T-20-60 DA decay time is shown in figure 14. Decay of the DA signal to between 20-60% of the maximum amount was approximately 70% longer in the control group (12.64±1.61 sec) than in the castrated animals (7.30±1.04 sec) in the NAc region ($p = 0.0070$). When compared to the DA decay time of K^+- treated castrated rats in the CPU (12.72±0.724), it took significantly less time in the NAc (7.30±1.039) to clear the DA concentration to 20-60% of the maximum ($p = 0.0031$). Comparisons between T-40-80 of K^+/Ctrl and K^+/CTX treatment groups in CPU and NAc are contained in figure 15. In the CPU, the T-40-80 lasted longer in the control than in the castrate group (21.6±0.969 versus 17.5±0.961), a statistical difference of $p = 0.0031$. Similarly, in the NAc, the amount of time required for the DA signal to decay to the 40-80% range was markedly shorter in the castrated (10.9±1.59) than in the intact animals (19.9±2.71), $p = 0.0046$. The two brain regions studied were shown to vary significantly ($p = 0.0069$) in the decay time in

the K^+/CTX groups, where DA 40-80 decay range was reached in less time in the NAc (17.5±0.961 versus 10.9±1.594). Figures 16 and 17 reveal no significant regional variations in the clearance rate and time course between the CPU and NAc or any changes due to the effects of castration.

DA release MPP^+/Ctrl versus MPP^+/CTX in CPU and NAc:

Contained in figures 18-25 is a comparison of analyzed MPP^+- evoked DA release characteristics in CPU and NAc of sham-castrated (MPP^+/Ctrl) and castrated (MPP^+/CTX) male rats. Differences in DA release were due to the effects of castration and were also dependent on brain regions. Figure 18 shows the comparison of DA release amplitude in the CPU and NAc of MPP^+-treated rats. The amount of DA released following MPP^+ infusion did not differ between sham-castrated and castrated animals in either the CPU or NAc. A significant difference was, however, found in DA amplitude between the CPU and NAc ($p = 0.0199$). The DA amplitude from the NAc of MPP^+/CTX was significantly suppressed when compared to the amplitude from CPU of MPP^+/CTX (0.289±0.0492 versus 0.511±0.0498 μM). The rise time, described in figure 19, was notably longer in CPU of castrated (34.6±1.79 sec) than in intact animals (27.4±1.06 sec), $p = 0.0003$. In the NAc, it also took substantially more time to secrete a maximal amount of DA in the MPP^+/CTX group (43.1±4.11 sec) when compared to the MPP^+/Ctrl animals (28.1±3.40 sec), $p = 0.0061$. A comparison between the CPU and NAc demonstrated a statistically significant difference ($p = 0.0314$), which showed that the rise time occurred more rapidly in CPU of castrates than in NAc of castrates (34.6±1.79 versus 43.1±4.11 sec). The DA secretion rate is depicted in figure 20. There were no distinctions observed between the two comparison groups in the CPU. On the contrary, the

secretion rate was notably reduced in the NAc of MPP^+/CTX with respect to MPP^+/Ctrl (19.03±2.71 versus 9.07±1.70 nM/sec), p = <0.0001, or when compared to the MPP^+/CTX in the CPU (18.83±1.91 nM/sec). The evaluation of the T-50 DA decay parameter (Figure 21) revealed that in the NAc considerably more time was required to decay DA concentration to the 50% time point in the MPP^+- treated castrated rats (134.6±15.96 sec) than in the intact controls (66.5±5.25 sec). This represents over a 100% difference in decay time (p =< 0.0001). Further, the T-50 decay time was also significantly longer in the MPP^+/CTX in the NAc when compared with the CPU (134.6±15.96 versus 83.0±4.63 sec), p =< 0.0001. When contrasting the T-20-60 decay values in intact controls and castrated animals, a statistically significant difference was shown in the NAc as illustrated in figure 22. The DA release was decayed to 20-60% of the maximal concentration much slower in the MPP^+/CTX (73.3±11.13 sec) than in the MPP^+/Ctrl group (36.1±5.47 sec). The calculated p-value of 0.0028 is equivalent to a 103% difference. Again, the effects of castration were more pronounced in the NAc than in the CPU. When comparing the castrate group in the NAc (73.3±11.13 sec) versus that in the CPU (41.6±5.22 sec), the DA signal decayed in a significantly longer time in the CPU of MPP^+ CTX animals (p = 0.0056). The T-40-80 parameter is presented in figure 23. The treatment groups in the CPU show a similar amount of time that it takes to reach the 40-80% time period. On the other hand, in the NAc, the 40-80 segment of the DA decay was again lengthened in the MPP^+/CTX group (121.6±30.90 versus 49.2±6.79 sec), p = 0.0183. A statistical difference (p = 0.0002) was also found with respect to brain regions. The T-40-80 DA decay time occurred markedly slower in the NAc of MPP^+- treated castrated

animals (121.6±30.90 sec) than in the CPU of MPP^+- treated castrated rats (50.3±3.96 sec). Figure 24 shows a comparison of DA clearance rate between the intact controls and castrated groups. In the NAc, the effects of castration produced a much slower DA clearance rate ($p = 0.0020$) in the MPP^+/CTX (2.61±0.539 nM/sec) when compared with the MPP^+/Ctrl (6.55±1.057 nM/sec) treatment group. The DA clearance rate occurred two times more slowly in the NAc of castrated animals (2.61±0.539 nM/sec) than in the CPU (7.17±0.708 nM/sec), $p = 0.0007$. Finally, figure 25 illustrates the DA time course results. Similar to other DA parameters analyzed in the CPU of intact and castrated groups, no statistically significant differences were observed between the groups in the total duration of the DA release event. However, in the NAc, the MPP^+ - induced DA release lasted for a significantly longer period of time in the MPP^+/CTX (321.9±41.9 sec) when compared to the MPP^+/Ctrl (193.2±25.5 sec) animals, $p = 0.0080$. Also, the results from the MPP^+/CTX subjects show a substantially longer time course in the NAc than in the CPU (321.9±41.9 versus 203.3±12.4 sec), $p = 0.0003$.

Figure 7. This figure illustrates a typical K^+- stimulated dopamine release from corpus striatum or nucleus accumbens. An asterisk is placed at the beginning of the release event. The y-axis represents micromolar concentrations of dopamine and the x-axis is given in seconds.

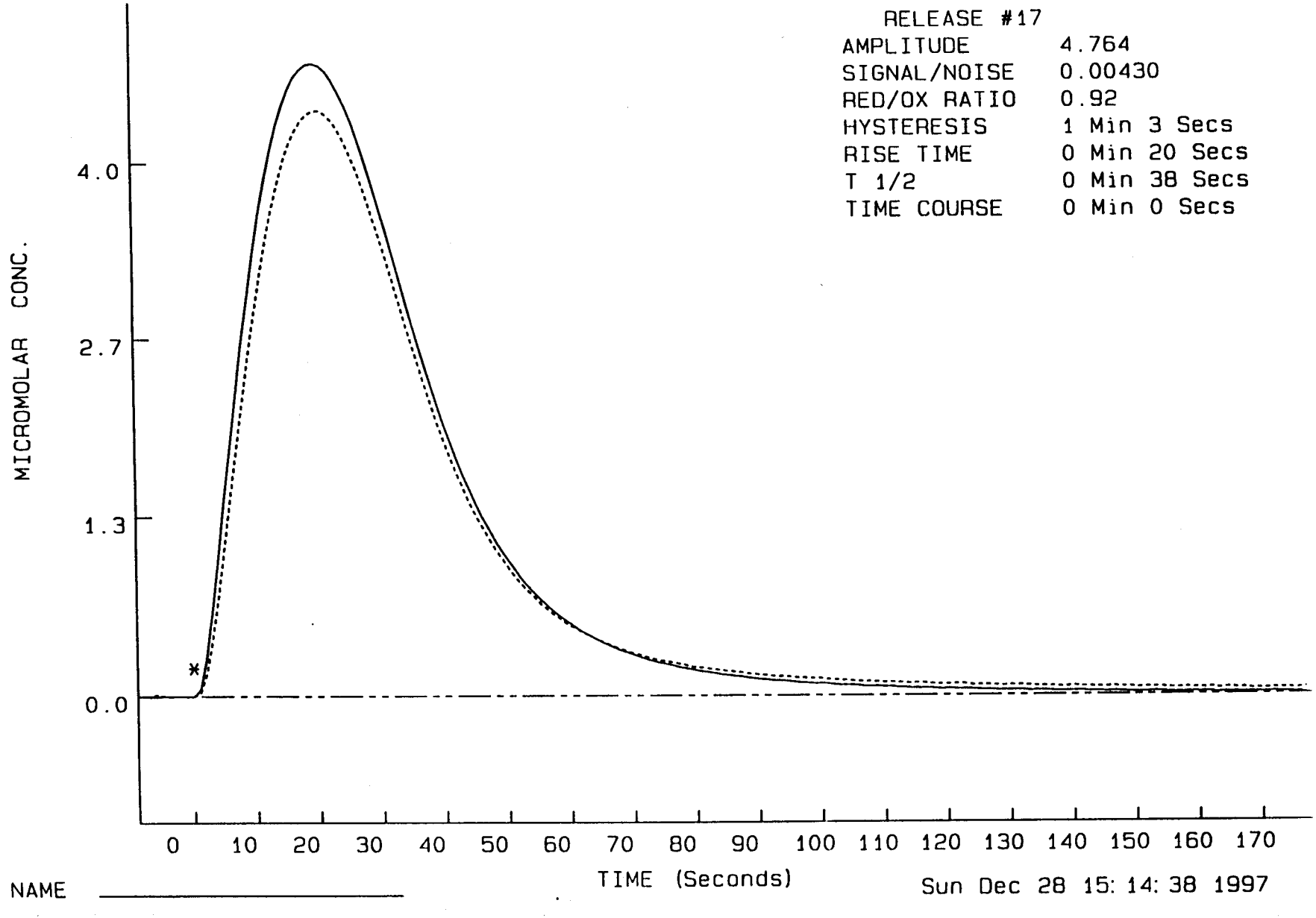
RELEASE #17
AMPLITUDE 4.764
SIGNAL/NOISE 0.00430
RED/OX RATIO 0.92
HYSTERESIS 1 Min 3 Secs
RISE TIME 0 Min 20 Secs
T 1/2 0 Min 38 Secs
TIME COURSE 0 Min 0 Secs
MICROMOLAR CONC.
4.0
2.7
1.3
0.0
0 10 20 30 40 50 60 70 80 90 100 110 120 130 140 150 160 170
TIME (Seconds)
NAME
Sun Dec 28 15: 14: 38 1997

Figure 8. This figure illustrates a typical dopamine release in response to MPP^+ infusion into corpus striatum or nucleus accumbens. An asterisk at the beginning marks the beginning of the recorded event and is plotted as function of micromolar concentrations of dopamine (y-axis) over time in seconds (x-axis).

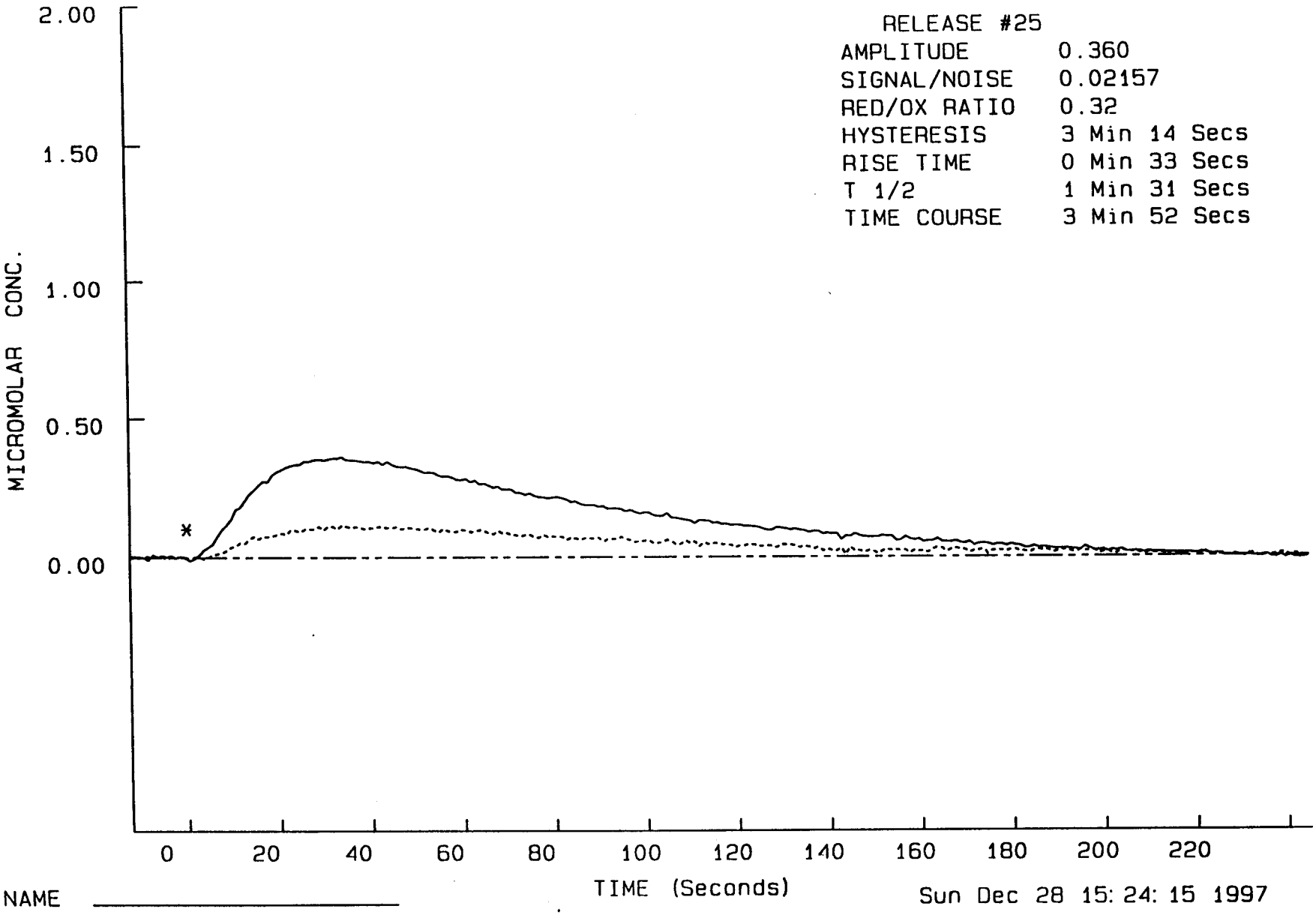
RELEASE #25
AMPLITUDE 0.360
SIGNAL/NOISE 0.02157
RED/OX RATIO 0.32
HYSTERESIS 3 Min 14 Secs
RISE TIME 0 Min 33 Secs
T 1/2 1 Min 31 Secs
TIME COURSE 3 Min 52 Secs
MICROMOLAR CONC.
2.00
1.50
1.00
0.50
0.00
0
20
40
60
80
100
120
140
160
180
200
220
TIME (Seconds)
NAME
Sun Dec 28 15: 24: 15 1997

Figure 9. This figure shows a comparison between potassium-stimulated dopamine release (top) and MPP^+- stimulated dopamine release (bottom).

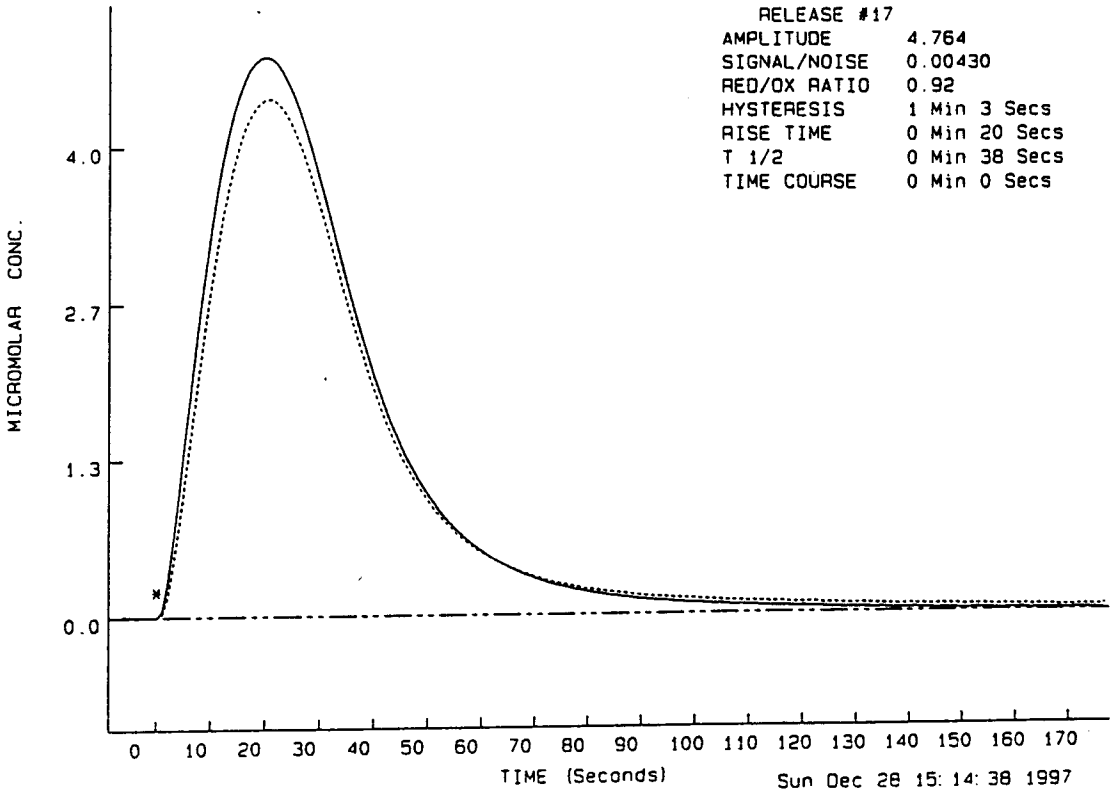
RELEASE #17
AMPLITUDE 4.764
SIGNAL/NOISE 0.00430
RED/OX RATIO 0.92
HYSTERESIS 1 Min 3 Secs
RISE TIME 0 Min 20 Secs
T 1/2 0 Min 38 Secs
TIME COURSE 0 Min 0 Secs
MICROMOLAR CONC.
4.0
2.7
1.3
0.0
0 10 20 30 40 50 60 70 80 90 100 110 120 130 140 150 160 170
TIME (Seconds)
Sun Dec 28 15:14:38 1997

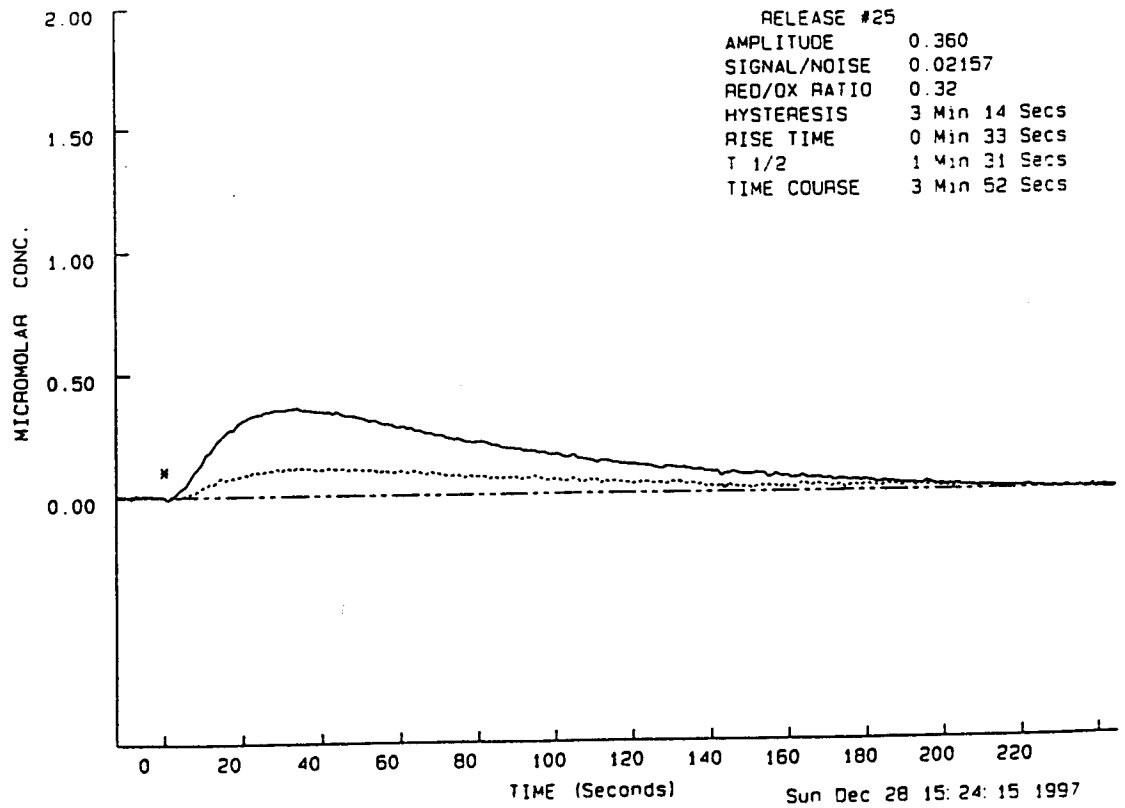
RELEASE #25
AMPLITUDE 0.360
SIGNAL/NOISE 0.02157
RED/OX RATIO 0.32
HYSTERESIS 3 Min 14 Secs
RISE TIME 0 Min 33 Secs
T 1/2 1 Min 31 Secs
TIME COURSE 3 Min 52 Secs
MICROMOLAR CONC.
2.00
1.50
1.00
0.50
0.00
0 20 40 60 80 100 120 140 160 180 200 220
TIME (Seconds)
Sun Dec 28 15:24:15 1997

Figure 10. Dopamine amplitude from corpus striatum (CPU) and nucleus accumbens (NAc) of K^+-treated intact (K^+ Ctrl) and castrated (K^+ CTX) male rats. Values reported in μM concentrations are expressed as the mean ± S.E.M. of n = 99 (K^+ Ctrl), n = 116 (K^+ CTX) in CPU; and n = 11 (K^+ Ctrl), and n = 20 (K^+ CTX) in NAc for figures 10-17.

(The following key is used to designate comparison groups analyzed statistically that were significantly different):

1 = K^+ Ctrl vs K^+ CTX in CPU

2 = K^+ Ctrl vs K^+ CTX in NAc

3 = K^+ Ctrl in CPU vs K^+ Ctrl in NAc

4 = K^+ CTX in CPU vs K^+ CTX in NAc

AMPLITUDE

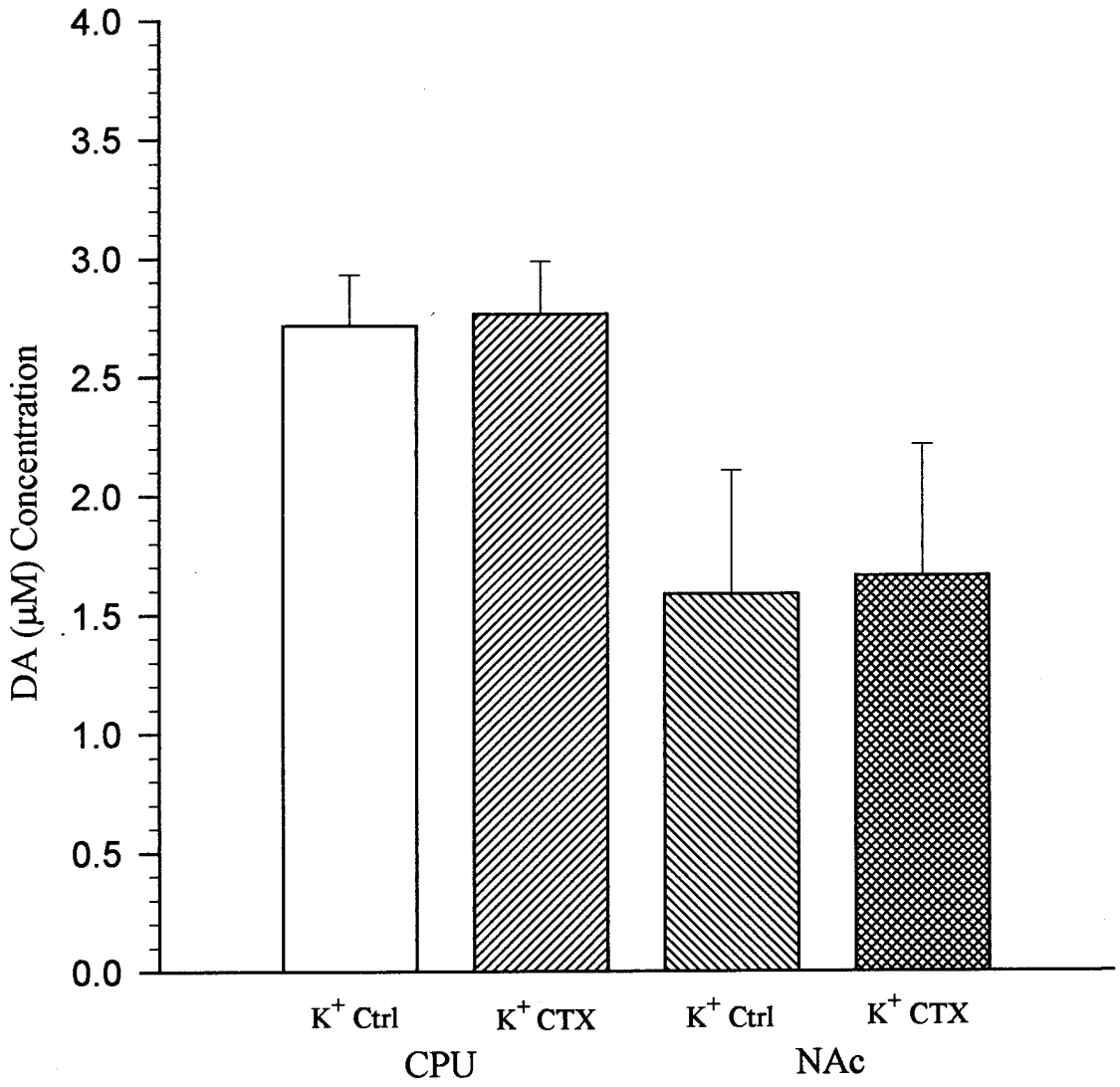
4.0
3.5
3.0
2.5
2.0
1.5
1.0
0.5
0.0
DA (μM) Concentration
K+ Ctrl
K+ CTX
K+ Ctrl
K+ CTX
CPU
NAc

Figure 11. Dopamine rise time in CPU and NAc of K^+-treated intact (K^+ Ctrl) and castrated (K^+ CTX) male rats. Values reported in seconds are the mean ± S.E.M.

4= ($p = 0.0188$) vs K^+ CTX (CPU)

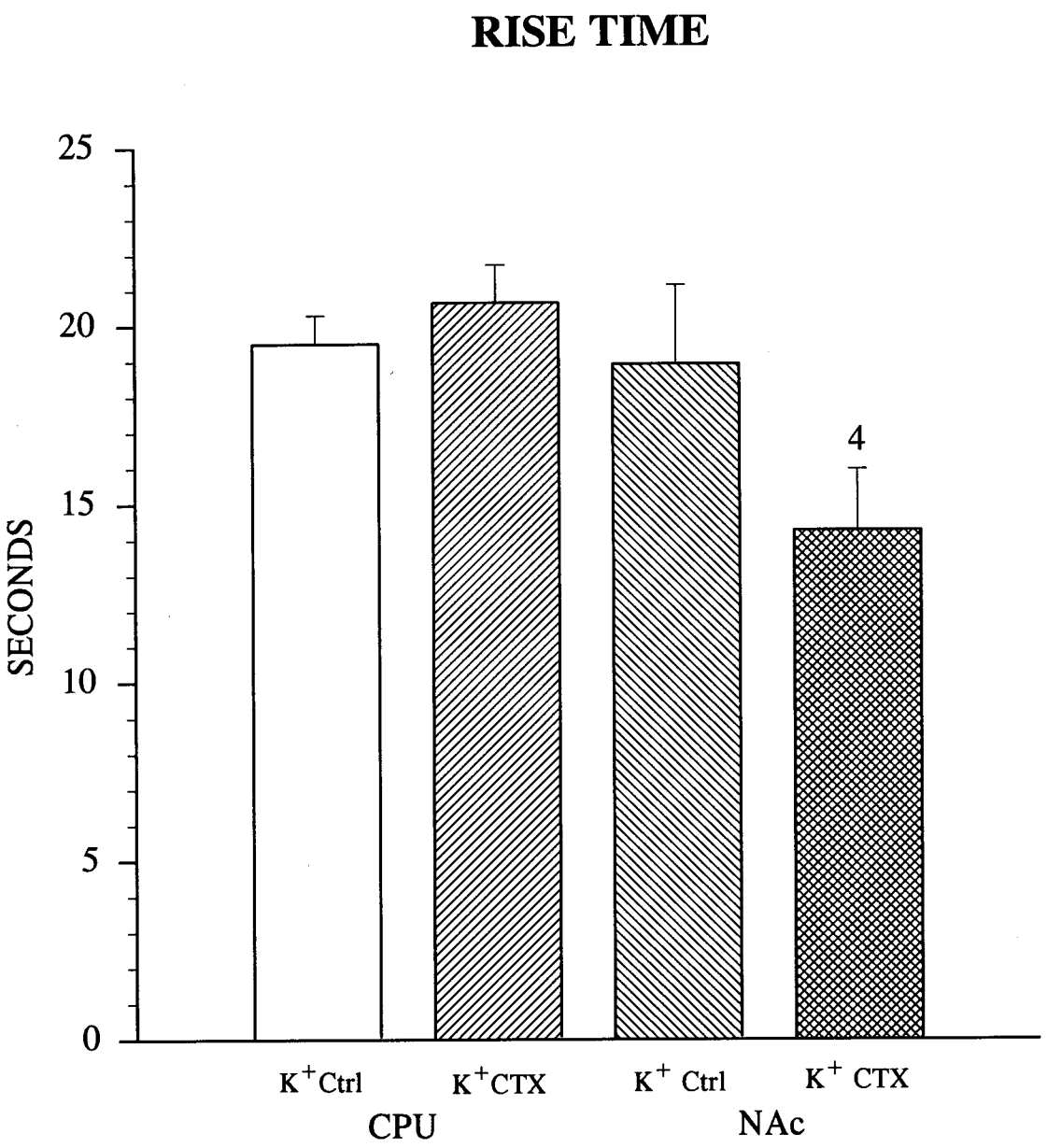
RISE TIME
25
20
15
10
5
0
SECONDS
4
K+Ctrl
K+CTX
K+ Ctrl
K+ CTX
CPU
NAc

Figure 12. Dopamine secretion rate in CPU and Nac of K^+- treated intact (K^+ Ctrl) and castrated (K^+ CTX) male rats. Values expressed in nanomolar per second (nM/sec) are the mean ±S.E.M.

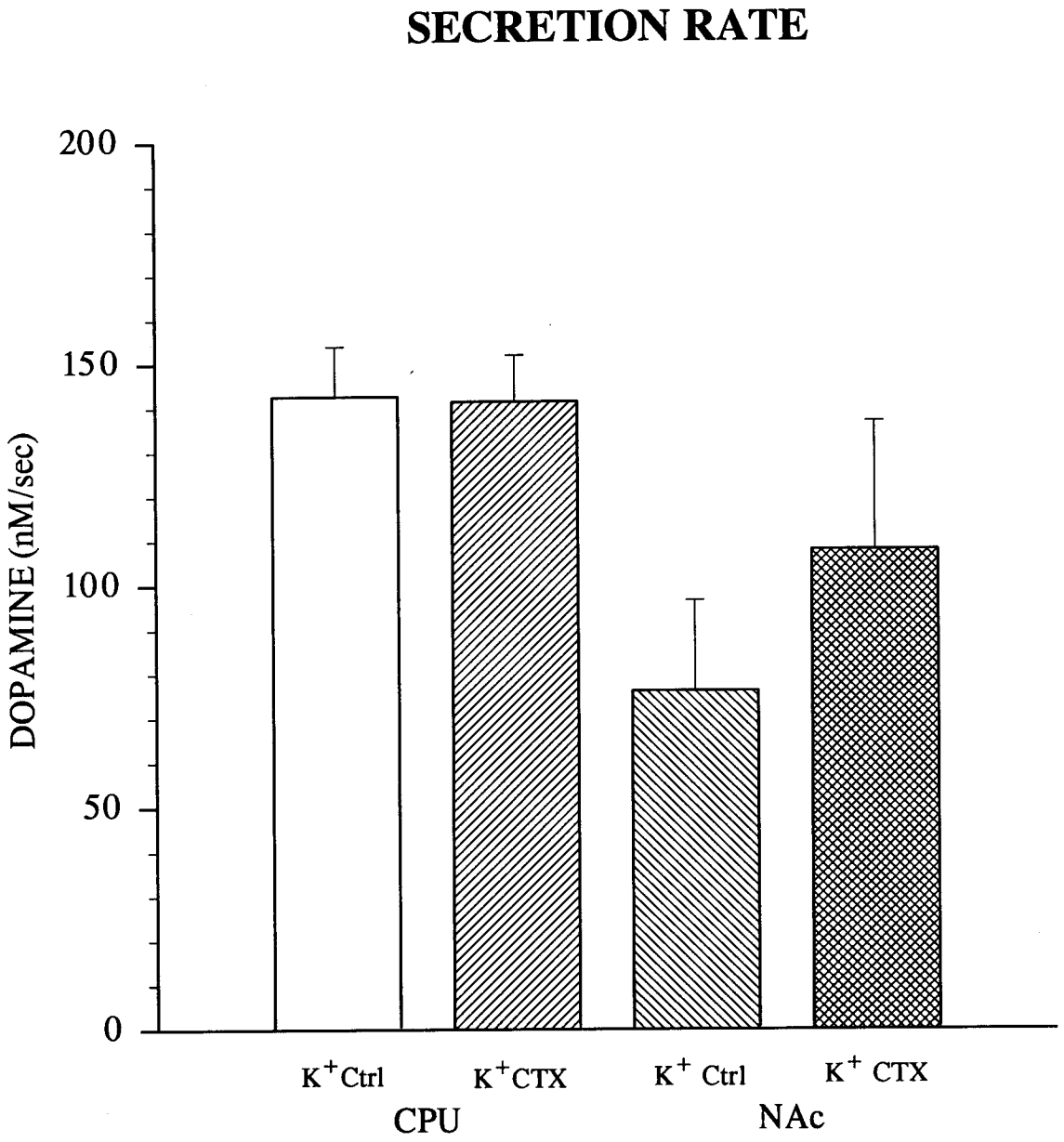
SECRETION RATE
200
150
100
50
0
DOPAMINE (nM/sec)
K+Ctrl
K+CTX
K+ Ctrl
K+ CTX
CPU
NAc

Figure 13. T-50, time for the dopamine signal to decay to 50% of peak value in CPU and NAc of K^+- treated intact (K^+ Ctrl) and castrated (K^+ CTX) male rats. Values reported in seconds are the mean ± S.E.M.

2 = (p = 0.0427) vs K^+ Ctrl (NAc)

4 = (p = 0.0107) vs K^+ CTX (CPU)

T - 50

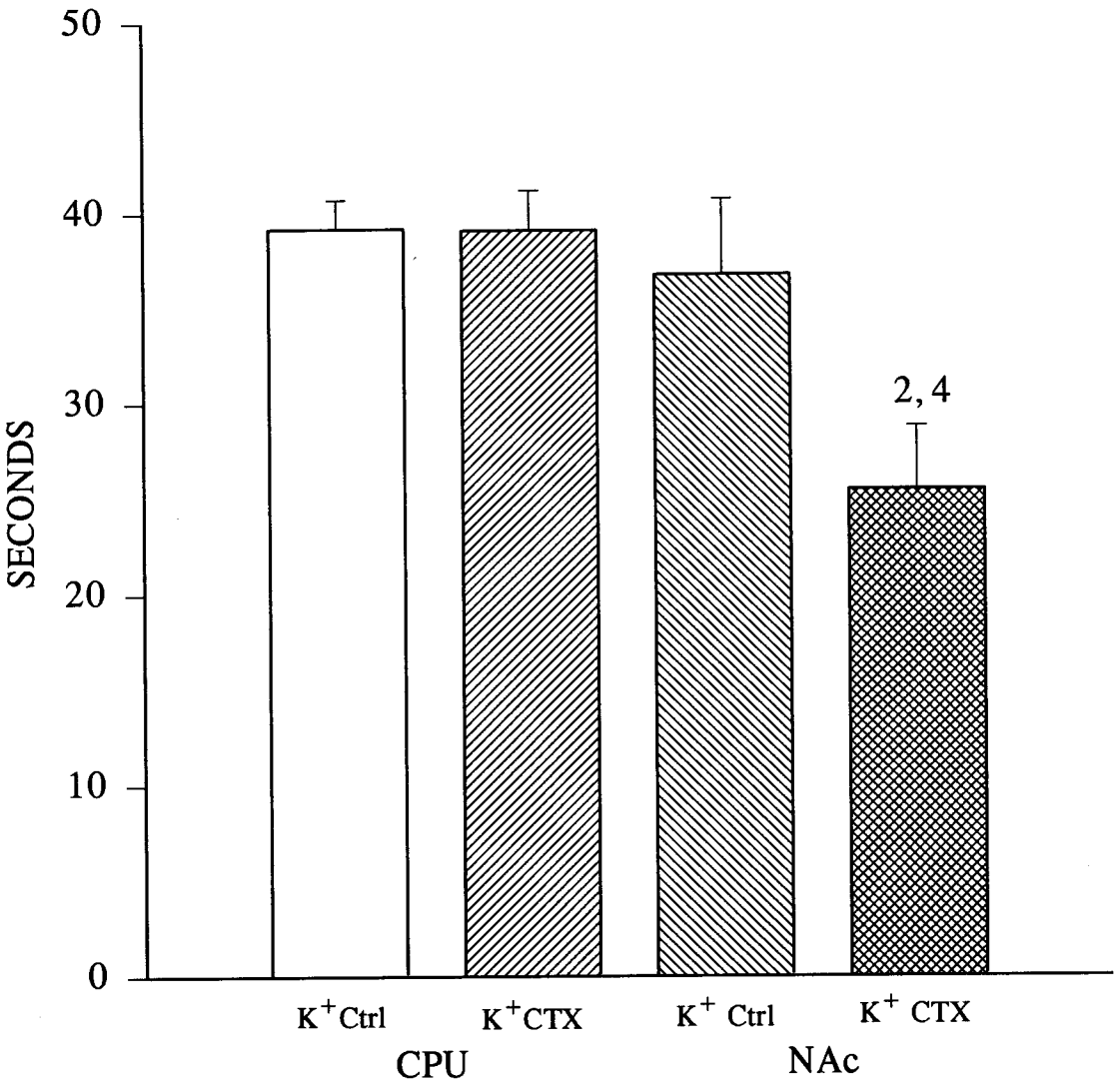

Figure 14. T-20-60, time for the dopamine signal to decay to 20-60% of peak value in CPU and NAc of K^+-treated intact (K^+ Ctrl) and castrated (K^+ CTX) male rats. Values reported in seconds are the mean ±S.E.M.

2 = ($p = 0.0070$) vs K^+ Ctrl (NAc)

4 = ($p = 0.0031$) vs K^+ CTX (CPU)

T - 20-60

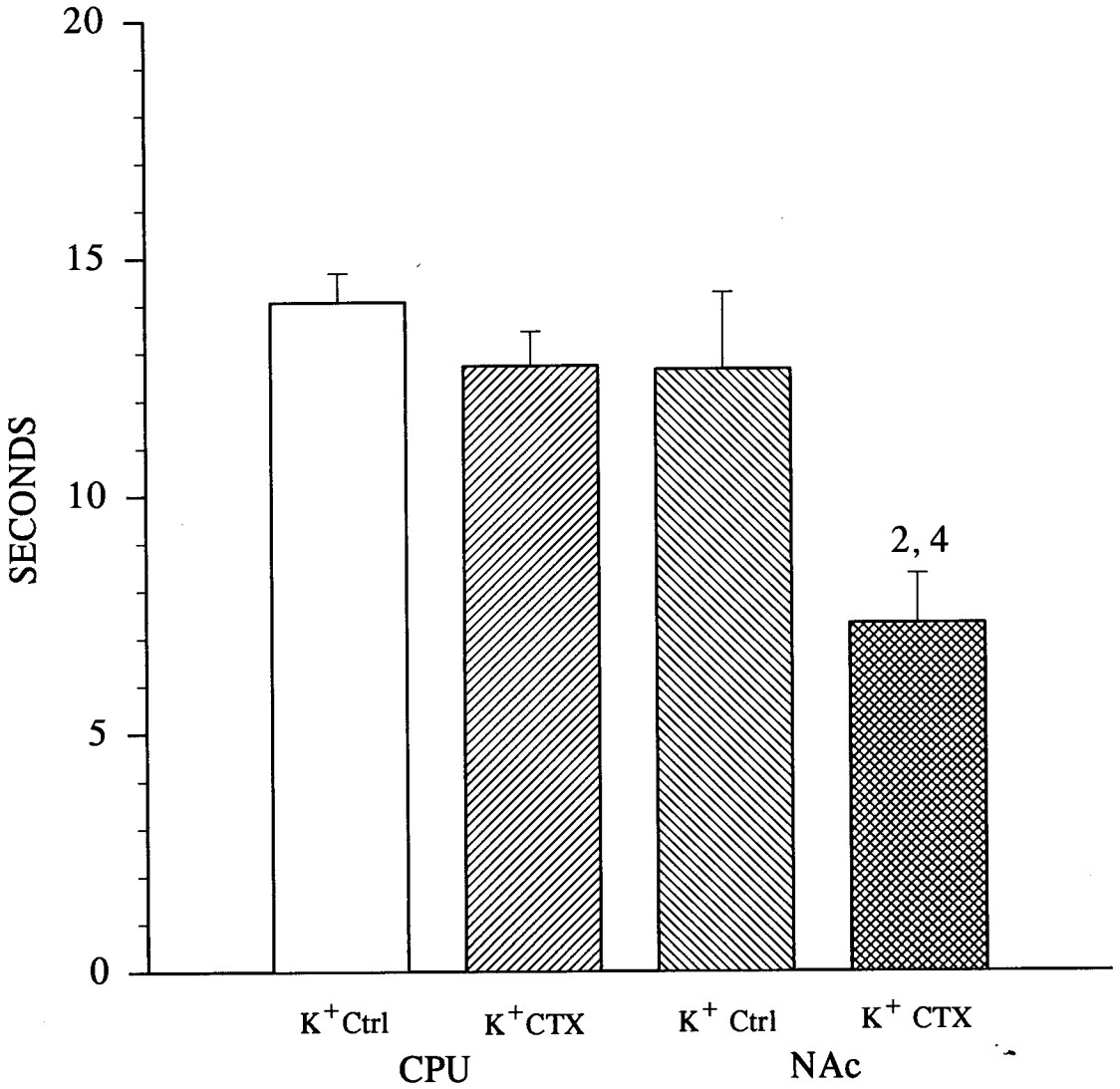

Figure 15. T-40-80, time for the dopamine signal to decay to 40-80% of peak value in CPU and NAc of K^+-treated intact (K^+ Ctrl) and castrated (K^+ CTX) male rats. Values expressed in seconds are the mean ± S.E.M.

1 = (p = 0.0031) vs K^+ Ctrl (CPU)

2 = (p = 0.0046) vs K^+ Ctrl (NAc)

4 = (p = 0.0069) vs K^+ CTX (CPU)

T - 40-80

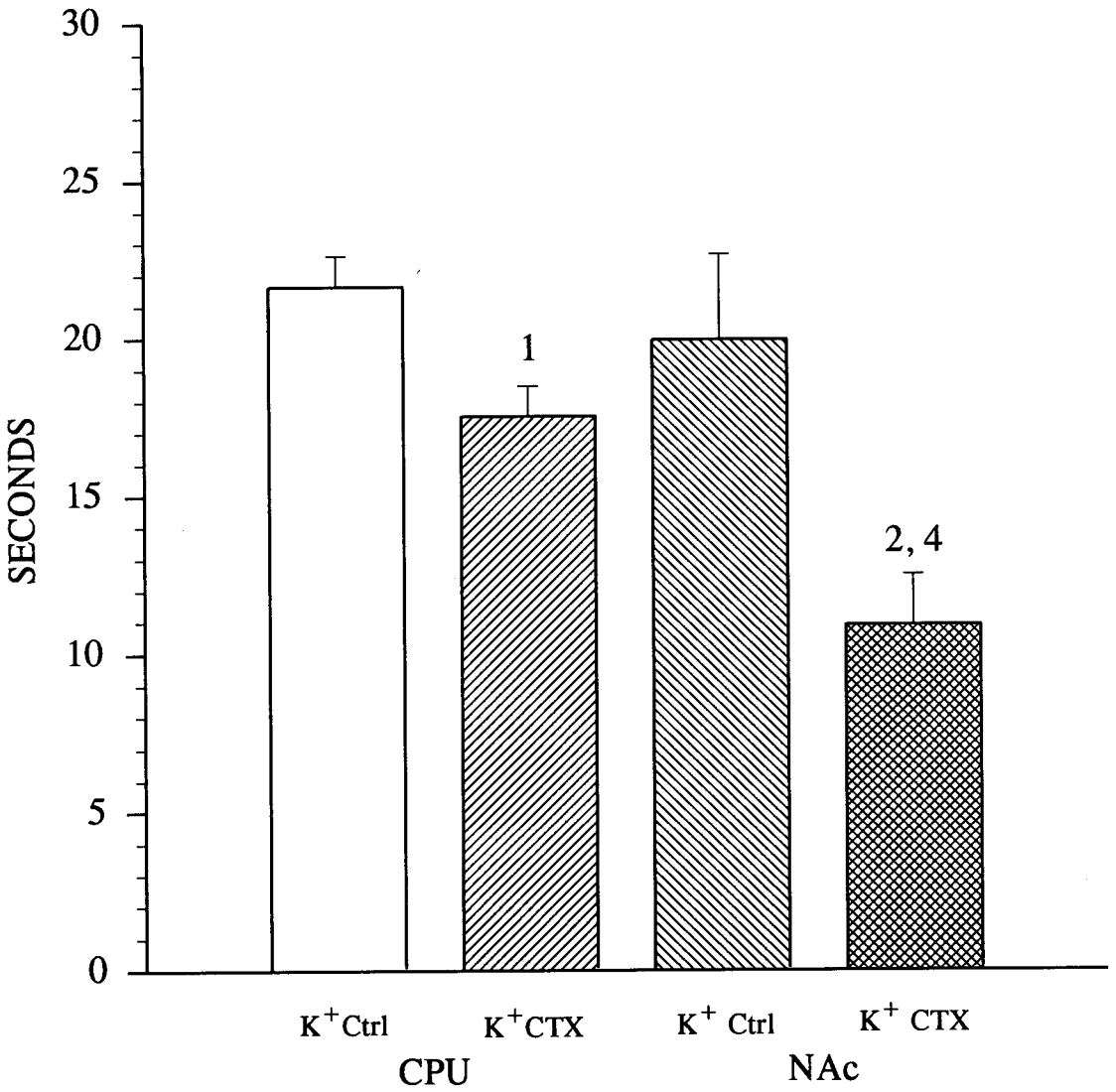

Figure 16. Dopamine clearance rate in CPU and NAc of K^+-treated intact (K^+ Ctrl) and castrated (K^+ CTX) male rats. Values reported in nM/sec are the mean ±S.E.M.

CLEARANCE RATE

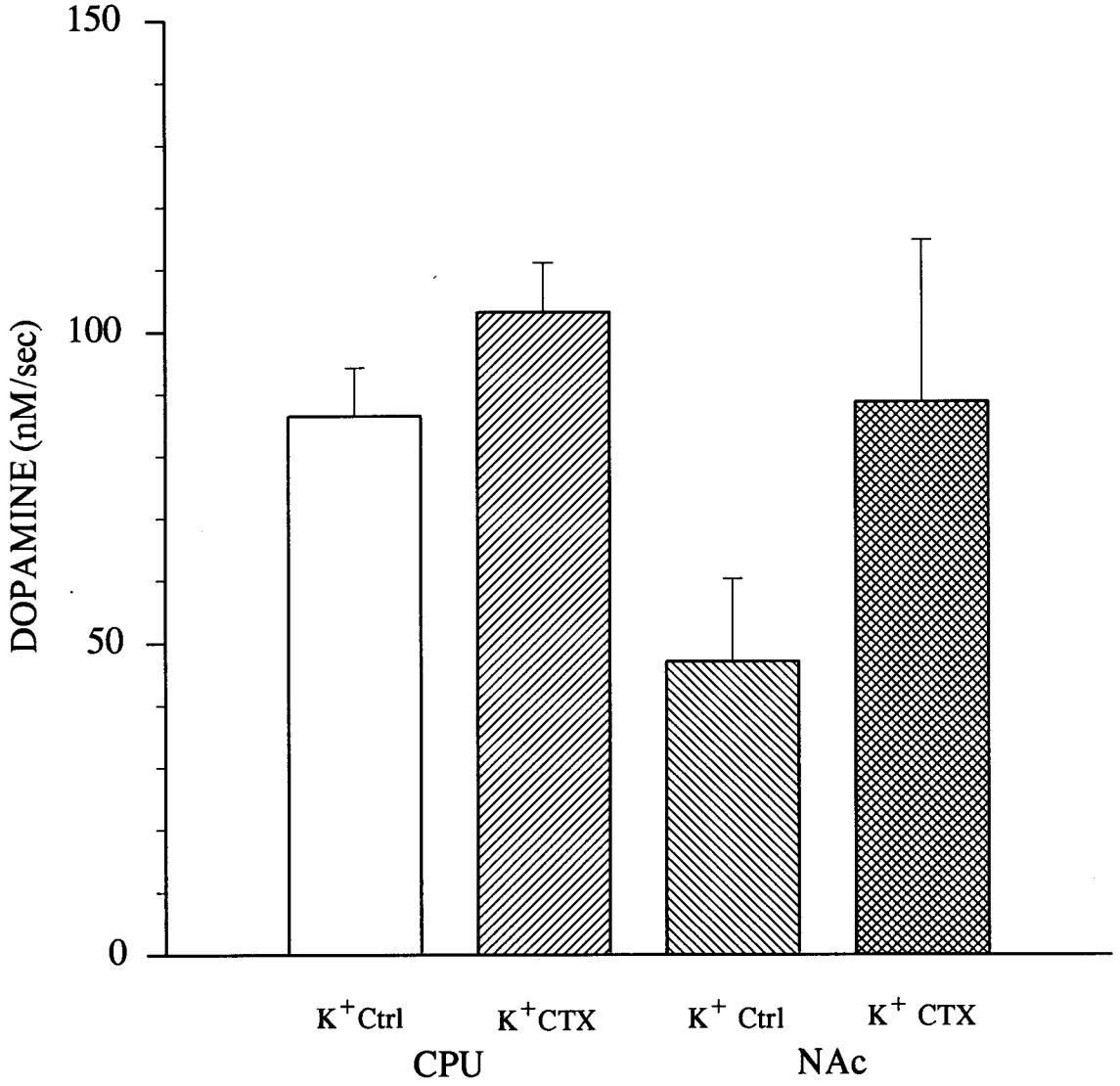

Figure 17. Time course of dopamine release from CPU and NAc of K^+-treated intact (K^+ Ctrl) and castrated (K^+ CTX) male rats. Values reported in seconds are the mean ± S.E.M.

TIME COURSE

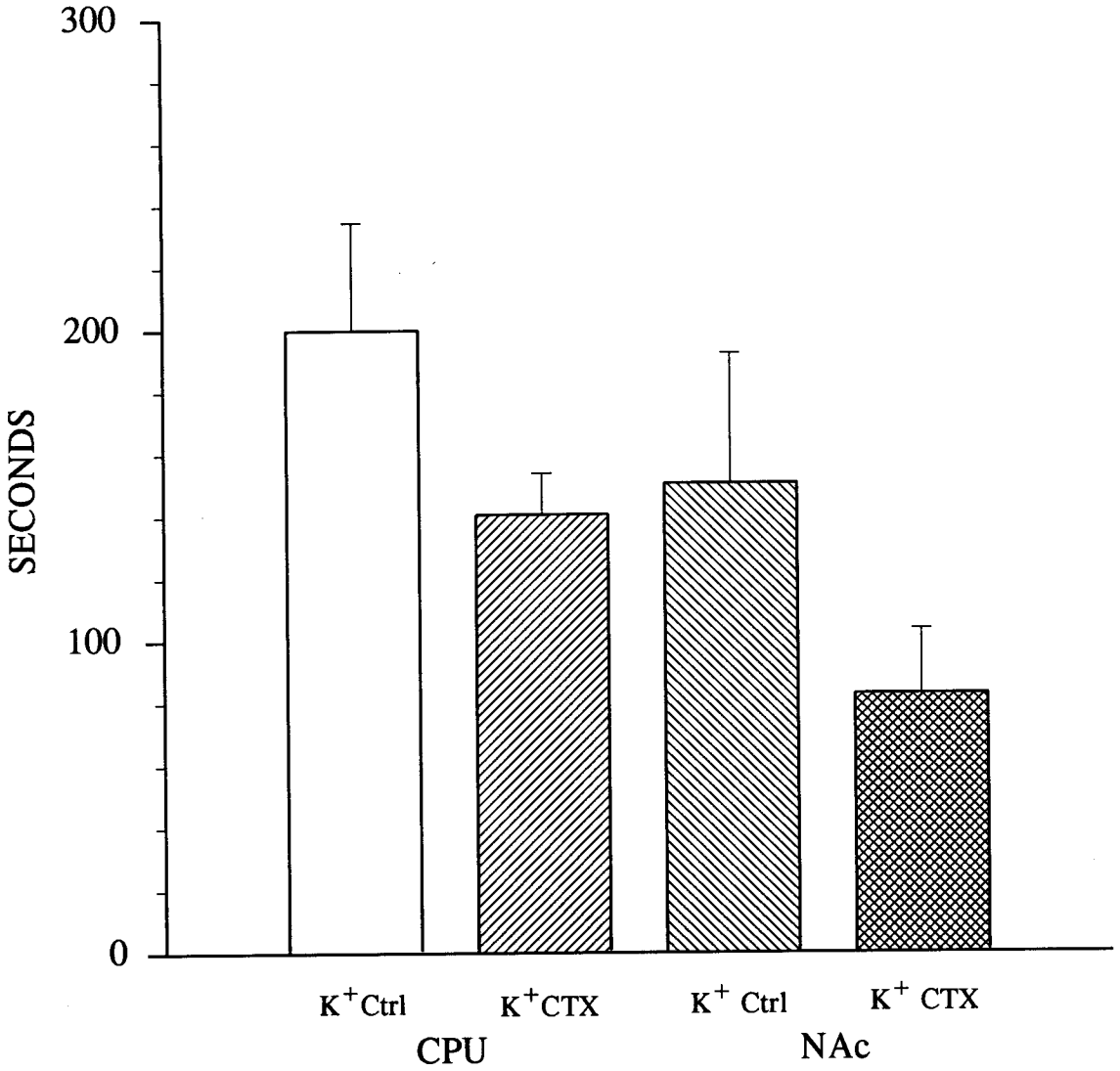

Figure 18. Dopamine amplitude from CPU and NAc of MPP^+-treated intact (MPP^+ Ctrl) and castrated (MPP^+ CTX) male rats. Values reported in μM concentrations are expressed as the mean ± S.E.M. of n = 143 (MPP^+ Ctrl), n = 101 (MPP^+ CTX) in CPU; and n = 34 (MPP^+ Ctrl), n = 31 (MPP^+ CTX) in NAc for figures 18-25.

4 = (p = 0.0199) vs MPP^+ CTX (CPU)

(The following key is used to designate comparison groups analyzed statistically that were significantly different):

1 = MPP^+ Ctrl vs MPP^+ CTX in CPU

2 = MPP^+ Ctrl vs MPP^+ CTX in NAc

3 = MPP^+ Ctrl vs MPP^+ Ctrl in CPU

4 = MPP^+ CTX vs MPP^+ CTX in NAc

AMPLITUDE

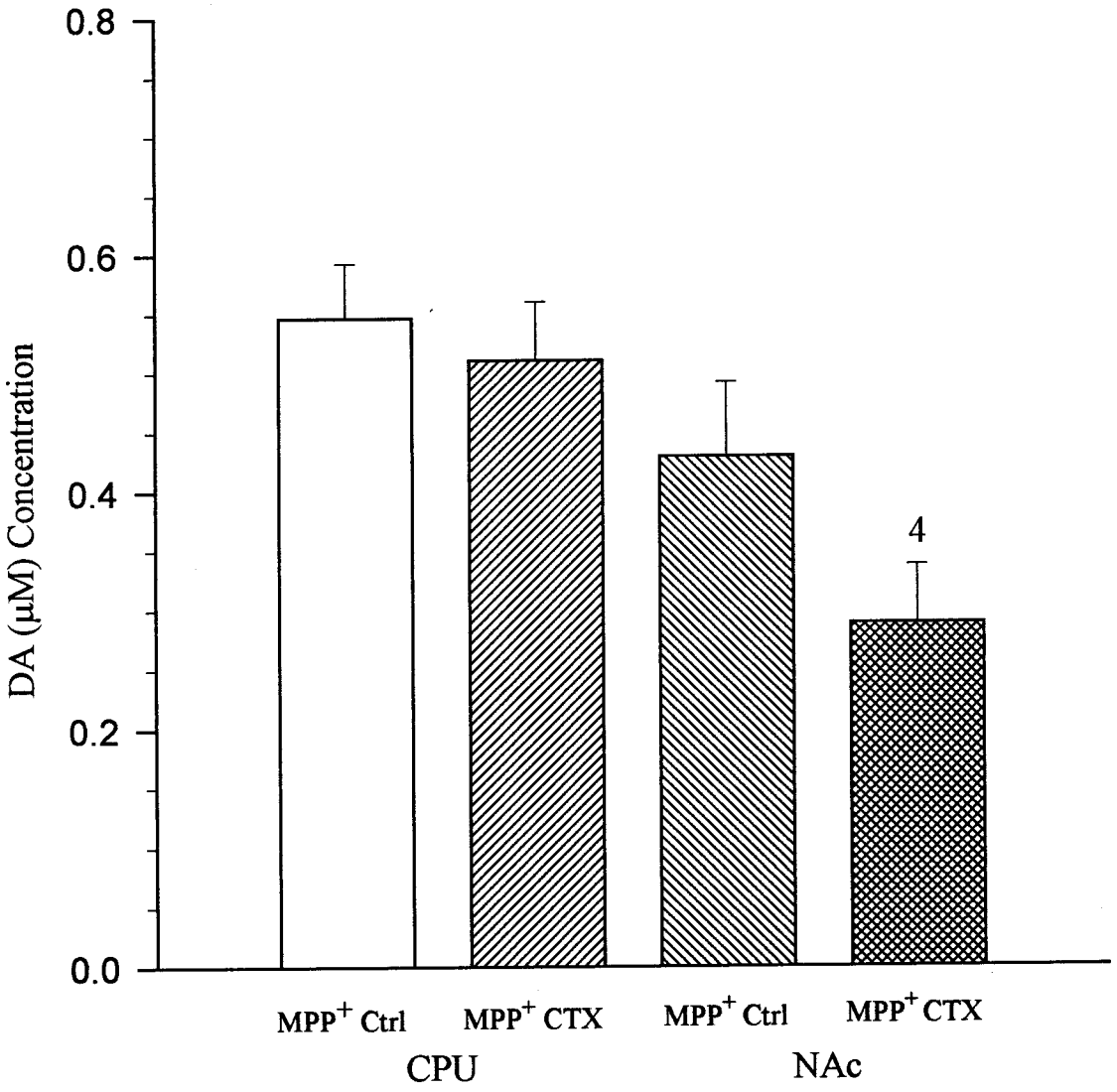
0.8
0.6
0.4
0.2
0.0
DA (μM) Concentration
4
MPP+ Ctrl
MPP+ CTX
MPP+ Ctrl
MPP+ CTX
CPU
NAc

Figure 19. Rise time of dopamine release in CPU and NAc of MPP^+-treated intact (MPP^+ Ctrl) and castrated (MPP^+ CTX) male rats. Values reported in seconds are the mean ± S.E.M.

1 = (p = 0.0003) vs MPP^+ Ctrl (CPU)

2 = (p = 0.0061) vs MPP^+ Ctrl (NAc)

4 = (p = 0.0314) vs MPP^+ CTX (CPU)

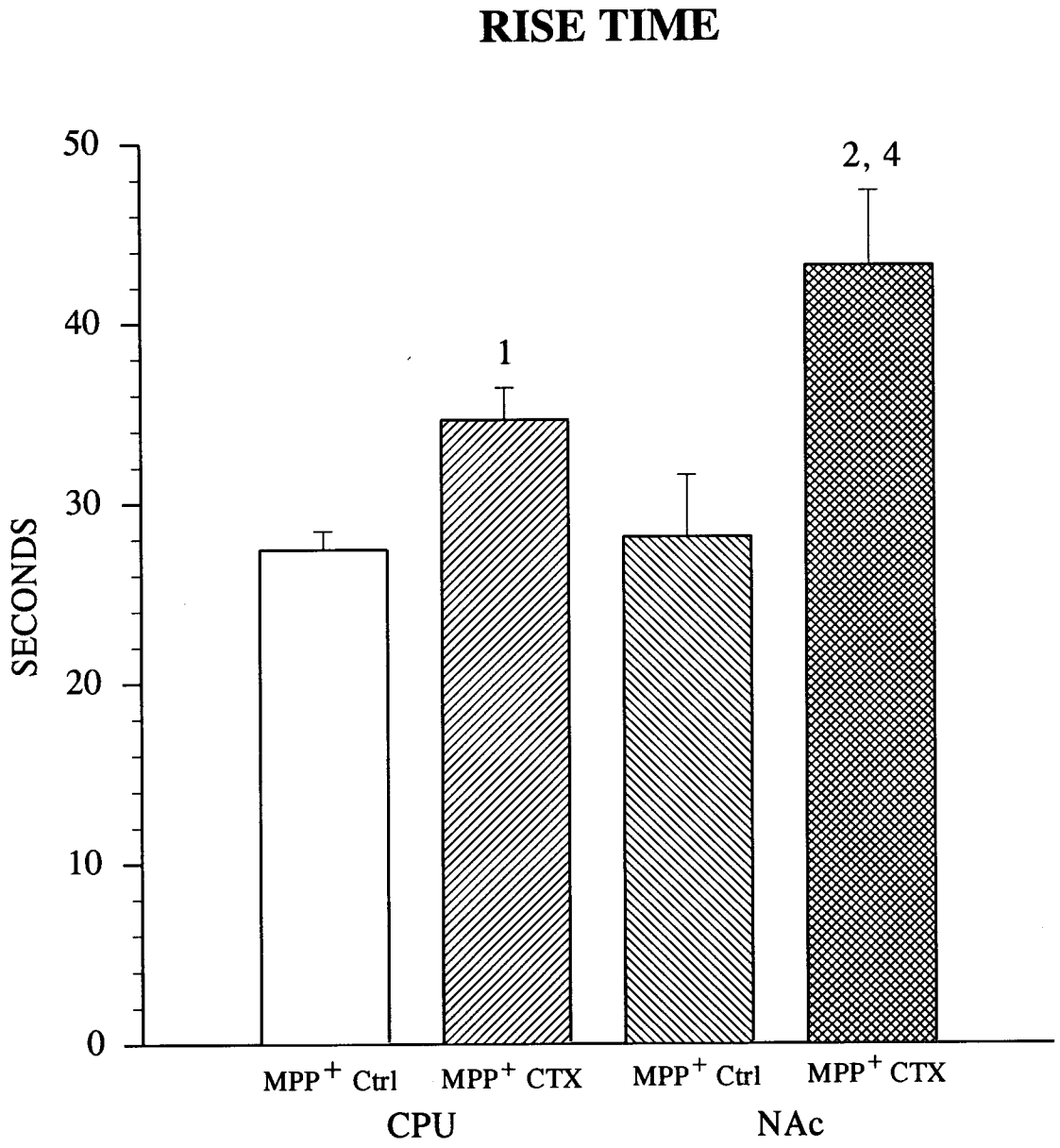
RISE TIME
50
40
30
20
10
0
SECONDS
1
2, 4
MPP+ Ctrl
MPP+ CTX
MPP+ Ctrl
MPP+ CTX
CPU
NAc

Figure 20. Dopamine secretion rate in CPU and NAc of MPP^+-treated intact (MPP^+ Ctrl) and castrated (MPP^+ CTX) in male rats. Values reported in nM/sec are expressed as the mean ± S.E.M.

2 = (p = 0.0034) vs MPP^+ Ctrl (NAc)

4 = (p = 0.0070) vs MPP^+ CTX (CPU)

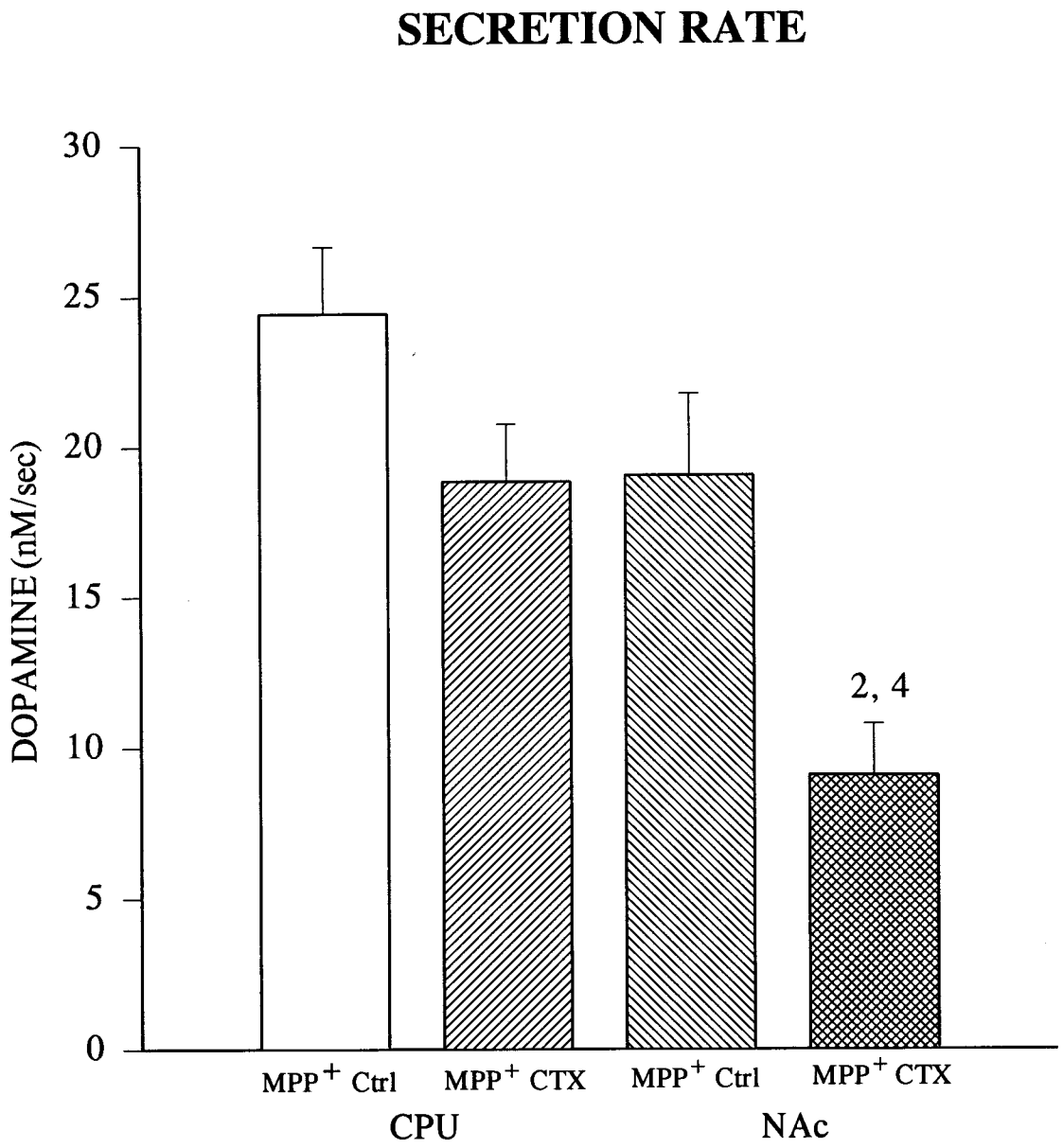
SECRETION RATE
DOPAMINE (nM/sec)
30
25
20
15
10
5
0
2, 4
MPP+ Ctrl
MPP+ CTX
MPP+ Ctrl
MPP+ CTX
CPU
NAc

Figure 21. T-50, time for the dopamine signal to decay to 50% of peak value in CPU and NAc of MPP^+-treated intact (MPP^+ Ctrl) and castrated (MPP^+ CTX) male rats. Values reported in seconds are the mean ± S.E.M.

2 = ($p = <0.0001$) vs MPP^+ Ctrl (NAc)

4 = ($p = <0.0001$) vs MPP^+ CTX (CPU)

T - 50

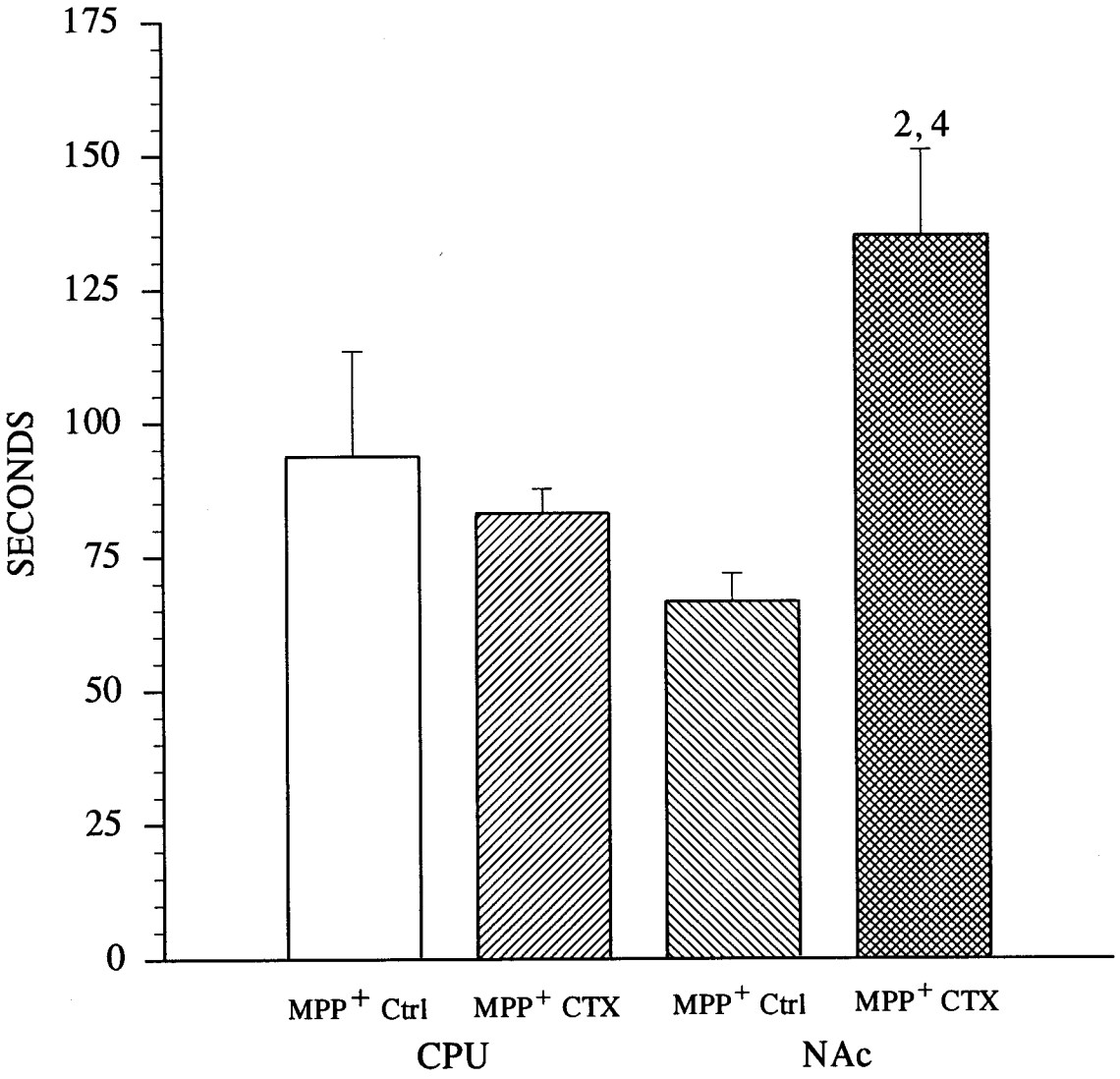
175
150
125
100
75
50
25
0
SECONDS
2, 4
MPP+ Ctrl
MPP+ CTX
MPP+ Ctrl
MPP+ CTX
CPU
NAc

Figure 22. T-20-60, time for the dopamine signal to decay to 20-60% of peak value in CPU and NAc of MPP^+-treated intact (MPP^+ Ctrl) and castrated (MPP^+ CTX) male rats. Values reported in seconds are the mean ± S.E.M.

2 = (p = 0.0028) vs MPP^+ Ctrl (NAc)

4 = (p = 0.0056) vs MPP^+ CTX (CPU)

T - 20-60

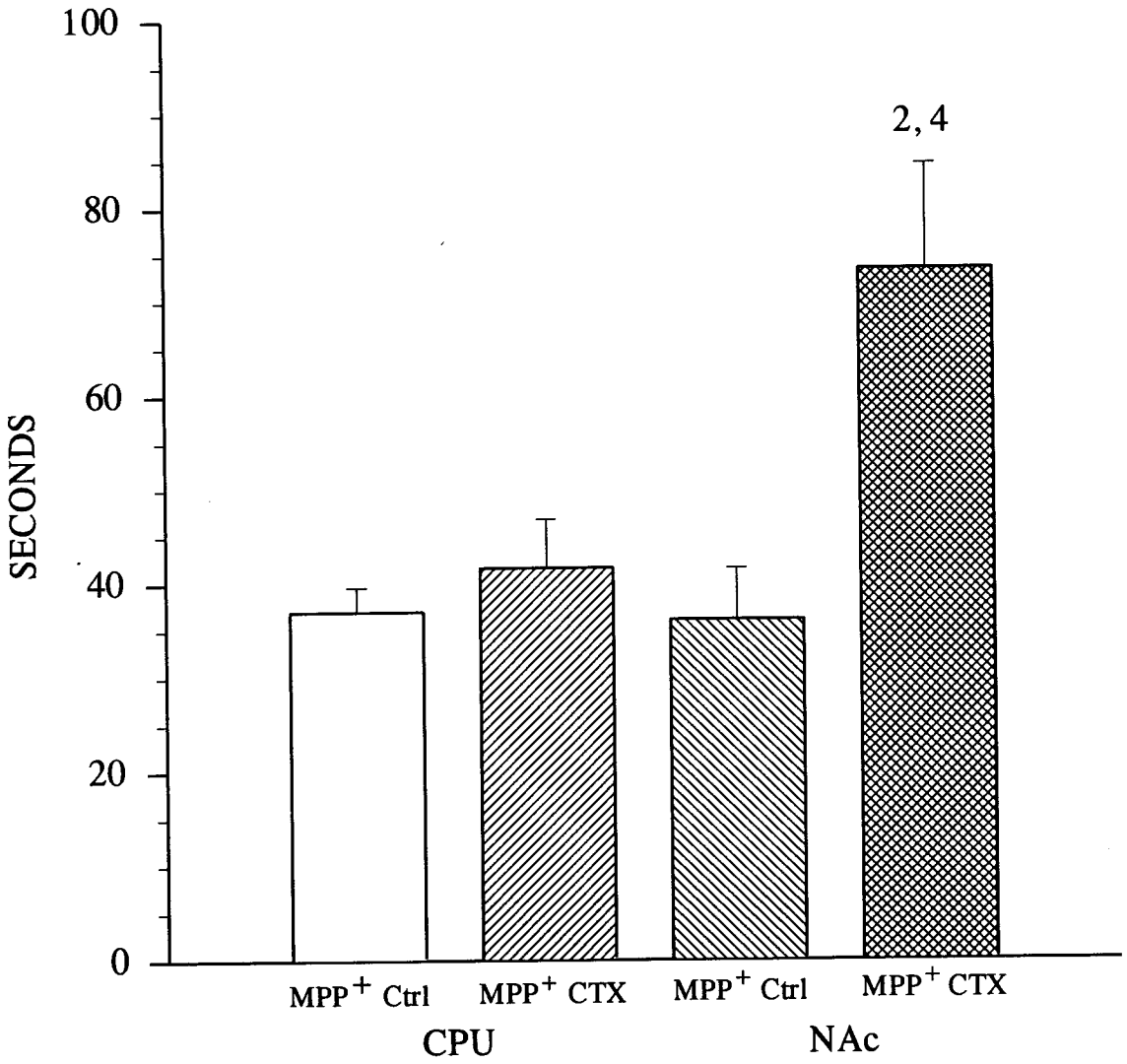
100
80
60
40
20
0
SECONDS
2, 4
MPP+ Ctrl
MPP+ CTX
MPP+ Ctrl
MPP+ CTX
CPU
NAc

Figure 23. T-40-80, time for the dopamine signal to decay to 40-80% of peak value in CPU and NAc of MPP^+-treated intact (MPP^+ Ctrl) and castrated (MPP^+ CTX) male rats. Values reported in seconds are the mean ± S.E.M.

2 = ($p = 0.0183$) vs MPP^+ Ctrl (NAc)

4 = ($p = 0.0002$) vs MPP^+ CTX (CPU)

T - 40-80

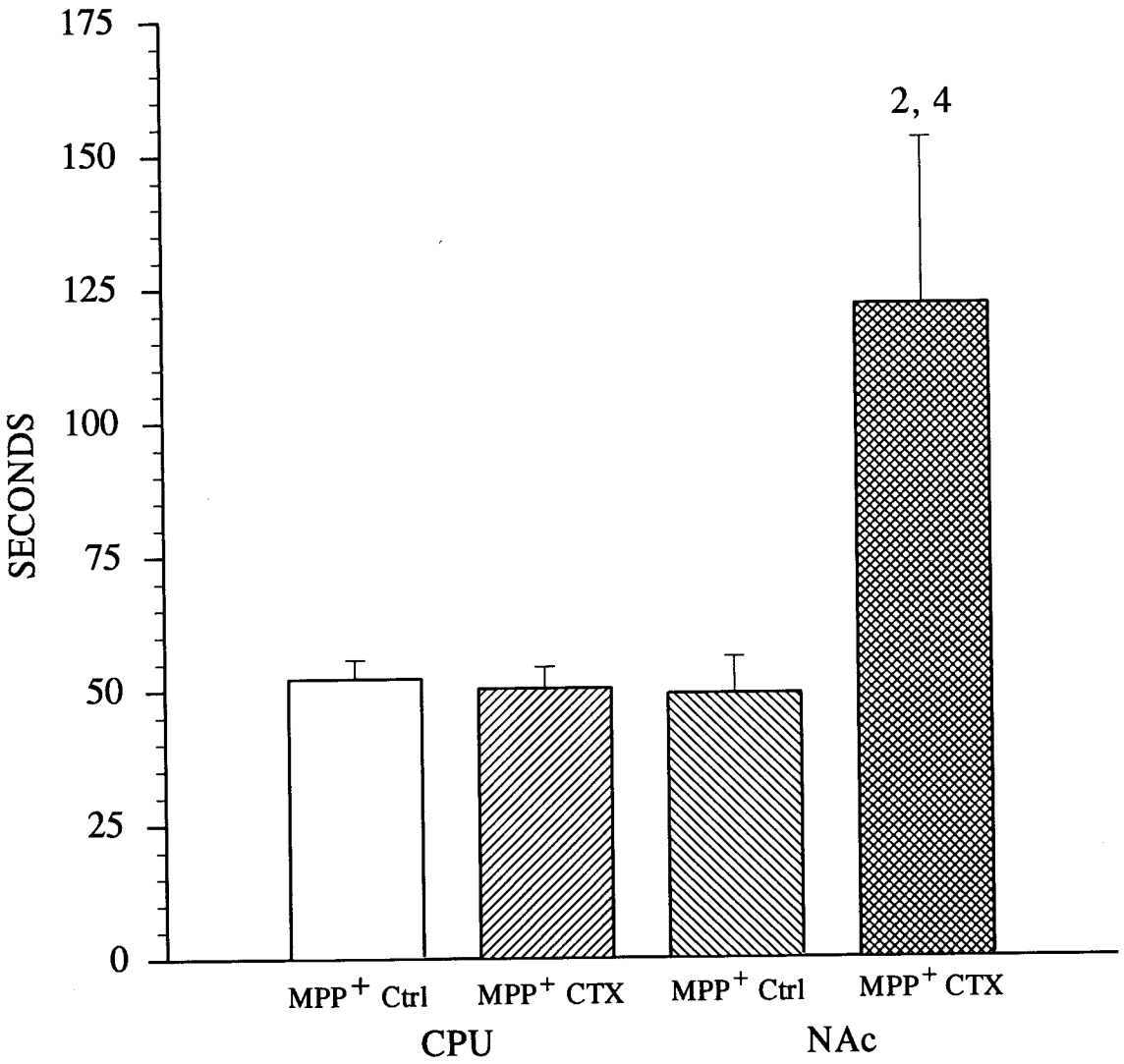
175
150
125
100
75
50
25
0
SECONDS
2, 4
MPP+ Ctrl
MPP+ CTX
MPP+ Ctrl
MPP+ CTX
CPU
NAc

Figure 24. Dopamine clearance rate in CPU and NAc of MPP^+-treated intact (MPP^+ Ctrl) and castrated (MPP^+ CTX) male rats. Values reported in nM/sec are the mean ± S.E.M.

2 = (p = 0.0020) vs MPP^+ Ctrl (NAc)

4 = (p = 0.0007) vs MPP^+ CTX (CPU)

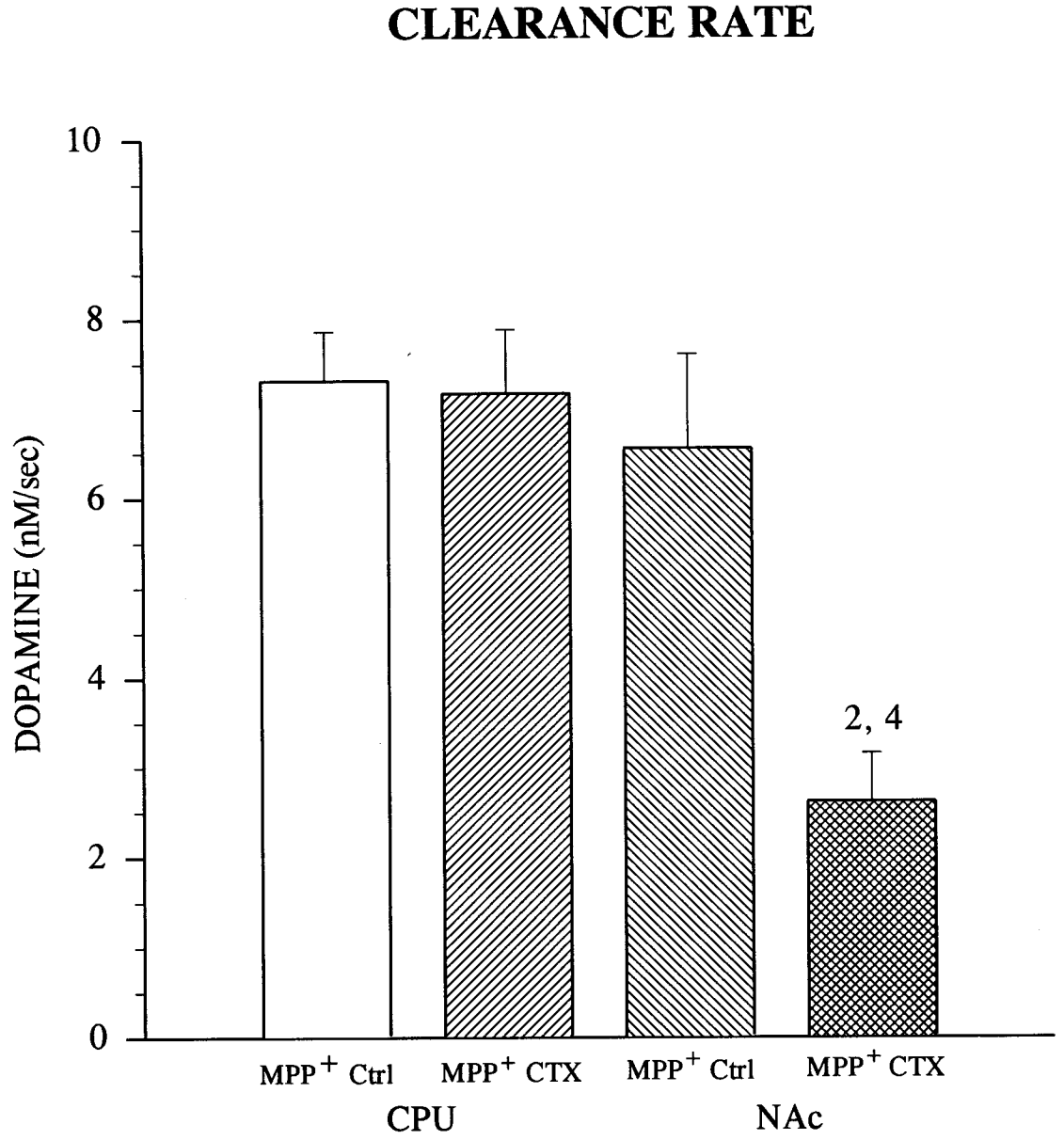
CLEARANCE RATE
DOPAMINE (nM/sec)
10
8
6
4
2
0
2, 4
MPP+ Ctrl
MPP+ CTX
MPP+ Ctrl
MPP+ CTX
CPU
NAc

Figure 25. Time courses of dopamine releases in CPU and NAc of MPP^+-treated intact (MPP^+ Ctrl) and castrated (MPP^+ CTX) male rats. Values reported in seconds are the mean ± S.E.M.

2 = (p = 0.0088) vs MPP^+ Ctrl (NAc)

4 = (p = 0.0003) vs MPP^+ CTX (CPU)

TIME COURSE

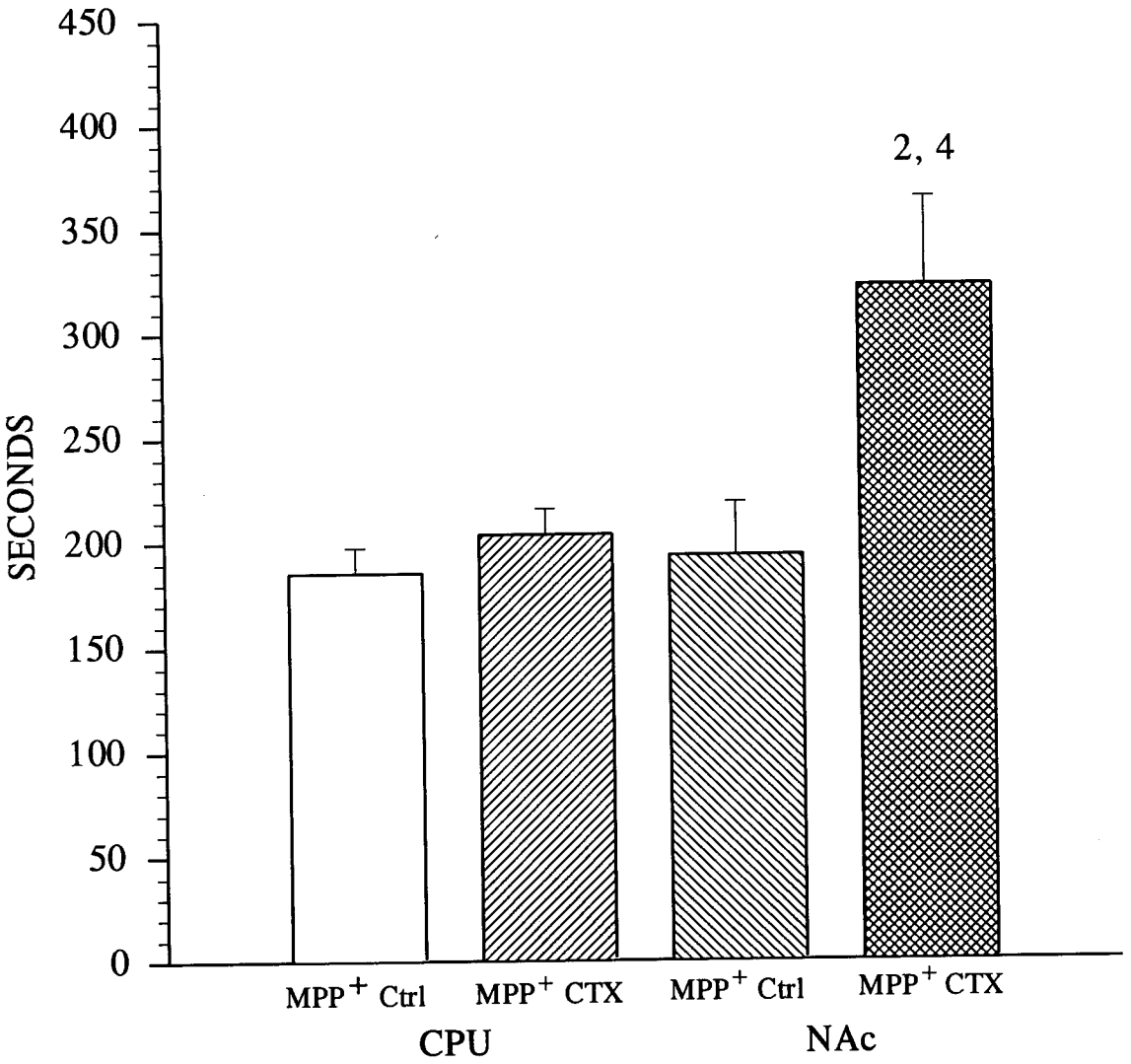
450
400
350
300
250
200
150
100
50
0
SECONDS
2, 4
MPP+ Ctrl
MPP+ CTX
MPP+ Ctrl
MPP+ CTX
CPU
NAc

CHAPTER 4

DISCUSSION:

The focus of this experiment was to investigate the effects of castration on the dynamics of acutely stimulated dopamine secretion by potassium and MPP^+. Corpus striatum and nucleus accumbens, brain areas receiving dopaminergic inputs from substantia nigra and ventral tegmental area, were studied for regional differences in androgen modulation of potassium and MPP^+- induced dopamine release characteristics.

Our results show clear differences in DA release and clearance parameters between K^+ and MPP^+ treatment as was expected based on previous *in vivo* studies performed in our laboratory using female rats (Arvin, 1998). These differences are due to the distinct mechanisms of action by which K^+ and MPP^+ affect the dopaminergic nerve terminals. There was a significant reduction in DA secretion rate following MPP^+ administration when compared to stimulation by potassium. A slow rise time, sometimes associated with a lag period before dopamine levels reached their maximum, was observed in MPP^+- treated animals, a finding similar to that reported by Chang and Ramirez (1986). Several hypotheses have been proposed which attempt to explain the process by which MPP^+ stimulates dopamine release. It has been demonstrated that MPP^+ binds intracellularly to dopamine storage vesicles in nigrostriatal nerve terminals (Del Zompo et al., 1992) and is thought to directly induce DA extravesiculation via the dopamine transporter (Chang and Ramirez, 1986). This is a process dramatically slower than the classical Ca^{++}- dependent exocytosis utilized by

K^+, which was demonstrated by the increased release of DA, faster secretion rate, and faster rise time of DA release following K^+ administration. The neurotoxic nature of MPP^+ was also well demonstrated by the clearance of the dopamine signal. The reduced clearance rate and longer DA signal decay times can be attributed to the fact that MPP^+, which has been shown to be selectively taken up into the striatal nerve terminals of rats (Irwin and Langston, 1985), competes with dopamine for uptake into the striatal synaptosomes by the dopamine transporter (Chiba et al., 1985; Javitch et al., 1985; Gerlach et al., 1991). Also important is the report by Scherman et al. (1988) which indicated that MPP^+ uptake into the vesicles, as is the case with dopamine, is an ATP-dependent process and therefore, could also contribute to the inhibition of dopamine clearance from the synapse and ultimately from the cytoplasm by depleting ATP stores. As dopamine is slowly being displaced from its storage vesicles into the synaptic cleft by MPP^+ and then is prevented from re-entering the terminal by MPP^+'s competition with dopamine at the transporter, the time required to clear dopamine from the synapse increases substantially. Indeed, the total duration of the DA signals recorded was significantly longer in releases stimulated by MPP^+ when compared to those evoked by potassium. Also, the finding that both DA secretion and clearance rates were drastically suppressed by MPP^+ action when compared to that of K^+, further substantiates the report by Chiba et al. (1985), which described corpus striatum as the brain area with highest MPP^+ uptake into synaptosomes. There was a thirteen-fold decrease in the clearance rate of dopamine as MPP^+ competed with dopamine for the same uptake mechanism by the DA transporter. As MPP^+ stimulates dopamine release and inhibits dopamine uptake, it increases the concentration of and prolongs the presence of dopamine in the synapse. Therefore, the

autoxidation of dopamine and subsequent generation of cytotoxic free radicals is substantially increased (Poirier et al., 1985). This increase in cytotoxic byproducts of dopamine metabolism could contribute to MPP^+'s acute neurotoxic effects on dopaminergic cells. The differences observed between the potassium and MPP^+ treatment groups were similar in the corpus striatum and nucleus accumbens brain regions. Such a displacement of dopamine and inhibition of re-uptake seen in this experiment, may contribute to development of Parkinson's disease (Chiba et al., 1985; Javitch et al., 1985; Gerlach et al., 1991)

Whereas the effects of castration were minimal with potassium treatment in the corpus striatum, the differences were more pronounced in the nucleus accumbens. In the nucleus accumbens, the lack of testosterone resulted in a significantly faster decay time of the DA signal than in the intact animals treated with potassium (Figures 12-15). This finding is supported by studies which showed that testosterone decreases dopamine metabolism in the rat striatum (Bitar et al., 1991) and decreases the overall activity of dopaminergic neurons (Engel et al., 1979). The fact that the amplitude of DA released, the rise time, and the secretion rate were not affected by castration indicates that testosterone does not influence the mode of action by which potassium stimulates dopamine release from nerve terminals in the corpus striatum and nucleus accumbens. In contrast, a study by Mitchell and Stewart (1989) demonstrated that castration lead to decreased dopamine levels in nucleus accumbens.

The effects of castration were more evident in the MPP^+ treatment groups. The corpus striatum is known to be a region rich in dopaminergic nerve terminals (Chiba et al., 1985) and showed a somewhat greater amplitude of dopamine release following MPP^+ treatment when compared to

the nucleus accumbens. However, no noticeable changes in DA release dynamics were revealed in the corpus striatum between the intact and castrated male rats. Thus the present results suggest that in the corpus striatum there is little, if any, androgen modulation of MPP^+- induced dopamine release. These results are supported by an *in vitro* study by Dluzen (1996) which reported the inability of testosterone to modulate dopaminergic neurotoxicity following MPTP treatment.

On the other hand, the effects of castration on dopamine release characteristics were much more evident in the nucleus accumbens than in the corpus striatum of MPP^+- treated rats. The dopamine secretion rate was significantly suppressed and rise time longer in the nucleus accumbens of castrated animals when compared to intact controls. Similarly, MPP^+ significantly reduced the clearance rate and subsequently prolonged the decay of the dopamine signal in the castrated animals. Thus, in the nucleus accumbens, in the absence of testosterone, MPP^+ was not able to stimulate dopamine to the extent in intact animals. Surprisingly, our results revealed that the effects of MPP^+ on dopamine secretion and clearance was more potent in the castrate group and was much more effective in nucleus accumbens than in the corpus striatum. The nucleus accumbens and corpus striatum of castrated animals varied significantly in all parameters of MPP^+-stimulated dopamine release that were analyzed. This finding leads us to speculate that the nucleus accumbens may be more susceptible to androgen modulation of dopamine release and to MPP^+ neurotoxicity than the corpus striatum. The nucleus accumbens possesses a high concentration of D_2 dopamine receptors of which the D_{2a} receptor subtype is located on the pre-synaptic nerve terminal (Kandel et al., 1991). Since MPP^+'s acute neurotoxic effects are likely linked to its actions on the dopamine transporter, the higher

concentration of D_{2a} autoreceptors present in the nucleus accumbens could render it more susceptible MPP^+'s acute neurotoxic effects. Estrogen has been demonstrated to regulate D_2 dopamine receptors in the nigrostriatal system (Le'vesque et al., 1988) and is known to affect dopamine release and clearance in the nucleus accumbens (Arvin, 1998). Therefore, it might not be surprising that testosterone may have modulatory effects in the nucleus accumbens. Whether or not there is a relationship between the effects of testosterone and MPP^+ on dopaminergic nerve terminal function remains to be determined. Future studies, in which dihydrotestosterone (DHT), a non-aromatizable metabolite of testosterone, and MPP^+ would be administered simultaneously by direct injection into the corpus striatum and nucleus accumbens, could provide additional information that might further strengthen and clarify the results from this study. Nevertheless, our current results indicate that testosterone may modulate the effectiveness of MPP^+-induced neurotoxicity on dopaminergic activity in the nucleus accumbens but not in the corpus striatum. Further investigations into the supposedly antidopaminergic role of testosterone (Engel et al., 1979; Dluzen et al., 1994; Dluzen et al., 1996b) will be required to aid in the determination of putative gender-related differences associated with Parkinson's disease.

SUMMARY:

In summary, the current results of this *in vivo* study clearly demonstrated the neurotoxic nature of MPP^+ when compared to potassium-treated controls. The significantly reduced secretion and clearance rates of dopamine demonstrated that MPP^+ and potassium act through different mechanisms to stimulate dopamine secretion, as well as support the theory

that MPP^+ hinders dopamine re-uptake by competing with the DA transporter. More importantly, our data suggest that testosterone modulates the dynamics of MPP^+- stimulated dopamine secretion in the nucleus accumbens. Furthermore, the nucleus accumbens revealed a significantly greater degree of responsiveness to androgen modulation than the corpus striatum. Additional investigation into the role of androgens in parts of the limbic system, like the nucleus accumbens, could provide important information, which may lead to a better understanding of the possible relationship between the motor symptoms of parkinsonism and brain areas involved with the cognitive aspects of motor behavior.

REFERENCES

Alfsen, A., (1983) Biophysical aspects of the mechanism of action of steroid hormones. Prog. Biophys. Mol. Biol., 42:79-93.

Arvin, M., Jr., (1998) Estrogen modulation of MPP^{+}-induced dopamine secretion in the corpus striatum and nucleus accumbens of the rat brain. M.S. Thesis, Youngstown State University.

Bacapoulos, N. J., Bhatnagar, R. K., (1977) Correlation between tyrosine hydroxylase activity and catecholamine concentration or turnover in brain regions. Journal of Neurochemistry, 29:639.

Becker, J. B., (1990a) Estrogen rapidly potentiates amphetamine-induced striatal dopamine release and rotational behavior during microdialysis. Neuroscience Letters, 118:169-171.

Becker, J. B., (1990b) Direct effect of 17beta-estradiol on striatum: Sex differences in dopamine release. Synapse, 5:157-164.

Bedard, P., Langelier, P., and Villeneuve, A., (1977) Oestrogens and extrapyramidal system. The Lancet, 1367-1368.

Bitar, M. S., Ota, M., Linnola, M., and Shapiro, B. H., (1992) Modification of gonadectomy-induced increases in brain monoamine metabolism by steroid hormones in male and female rats. Psychoneuroendocrinilogy, 16:547-557.

Blaustein, J. D., (1986) Steroid receptors and hormones action in the brain. Ann. NY Acad. Sci., 474:400-414.

Bradbury, A. J., Costall, B., Domeney, A. M., Jenner, P. J., Marsden, C. D., Naylor, R. J., (1986) 1-Methyl-4-phenylpyridine is neurotoxic to the nigrostriatal dopamine pathway. Nature, 319:56-57.

Chang, G.D., Ramirez, V.D., (1986) The mechanism of action of MPTP and MPP^+ on endogenous dopamine release from the rat corpus striatum superfused *in vivo*. Brain Research, 368:134-140.

Chiasson, R.B., Laboratory Anatomy of the White Rat. 5th Ed., Wm. C. Brown Publishers, Dubuque, Iowa. 1988, pp. 4.

Chiba, K., Trevor, A., Castagnoli, Jr., N., (1984) Metabolism of the neurotoxic tertiary amine, MPTP, by brain monoamine oxidase. Biochemical and Biophysical Research Communications, 120:574-578.

Chiba, K., Trevor, A., Castagnoli, Jr., N., (1985) Active uptake of MPP^+, a metabolite of MPTP, by brain synaptosomes. Biochemical and Biophysical Research Communications, 128:1228-1232.

Chiueh, C. C., Markey, S. P., Burns, R. S., Johannessen, J. N., Pert, A., Kopin, I. J., (1984) neurochemical and behavioral effects of systemic and intranigral administration of N-Methyl-4-Phenyl-1,2,3,6-tetrahydropyridine in the rat. European Journal of Pharmacology, 100:189-194.

Cooper, J. R., Bloom, F. E., Roth, R. H., The Biochemical Basis of Neuropharmacology. 5th Ed. Oxford, New York, Oxford University Press, 1986.

Corsini, G. U., Pintus, S., Chiueh, C. C., Weiss, J. F., Kopin, I. J., (1985) 1-Methyl-4-phenyl-1,2,3,6-tetrahydropyridine (MPTP) neurotoxicity in mice is enhanced by pretreatment with diethyldithiocarbamate. European Journal of Pharmacology, 119:127.

Crowley, W. R., O'Donohue, T. L., Jacobowitz, D. M., (1978) Sex differences in catecholamine content in discrete brain nuclei of the rat: effects of neonatal castration or testosterone treatment. Acta Endocrinologica, 89:20-28.

D'Amato, R. J., Lipman, Z. P., Snyder, S. H., (1986) Selectivity of parkinsonian neurotoxin MPTP: toxic metabolite MPP^+ binds to neuromelanin. Science, 231:987-989.

DelZompo, M., Ruiu, S., Maggio, R., Piccardi, M. P., Corsini, G. U., (1990) (^3H) 1-methyl-4-phenyl-2,3-dihydropyridinium ion binding sites in mouse brain: pharmacological and biological characterization. Journal of Neurochemistry, 54:1905-1910.

Del Zompo, M., Piccardi, M. P., Ruiu, S., Corsini, G. U., Vaccari, A., (1992) Characterization of a putatively vesicular binding site for [^3H] MPP^+ in mouse striatal membranes. Brain Research, 571:354-357.

Diamond, S. G., Markham, C. H., Hoehn, M. M., McDowell, F. H., Muenter, M. D., (1990) An examination of male-female differences in progression and mortality of Parkinson's disease. Neurology, 40:763-766.

DiMonte, D., Irwin, I., Kupsch, A., Cooper, S., DeLanney, L. E., Langston, J. W., (1989) Diethyldithiocarbamate and disulfram inhibit MPP^+ and dopamine uptake by striatal synaptosomes. European Journal of Pharmacology, 166:23.

DiMonte, D., Jewell, S. A., Ekstrom, G., Sandy, M. S., Smith, M. T., (1986) 1-Methyl-4-phenyl-1,2,3,6-tetrahydropyridine (MPTP) and 1-methyl-4-phenylpyridine (MPP^+) cause rapid ATP depletion in isolated hepatocytes. Biochem. Biophys. Res. Commun., 137:310.

Dluzen, D. E., McDermott, J. L., Liu, B., (1996a) Estrogen alters MPTP-induced neurotoxicity in female mice: effects on striatal dopamine concentrations and release. Journal of Neurochemistry, 66:658-666.

Dluzen, D. E., (1996b) Effects of testosterone upon MPTP-induced neurotoxicity of the nigrostriatal dopaminergic system of C57/ B1 mice. Brain Research, 12135:

Dluzen, D., Jain, R., Liu, B., (1994) Modulatory effects of testosterone on 1-methyl-4-phenyl-1,2,3,6-tetrahydropyridine-induced neurotoxicity. Journal of Neurochemistry, 62:94-101.

Dluzen, D. E., Ramirez, V. D., (1989) Progesterone effects upon dopamine release from the corpus striatum of female rats. II. Evidence for a membrane site of action and the role of albumin. Brain Research, 476:338-344.

Dluzen, D. E., Ramirez, V. D., (1984) Bimodal effect of progesterone on in vitro dopamine function of the rat corpus striatum. Neuroendocrinology, 39:149-155.

Engel, J., Ahlenius, S., Almgren, O., Carlsson, A., Larsson, K., Sodersen, P., (1979) Effects of gonadectomy and hormone replacement on brain monoamine synthesis in male rats. Pharmacology Biochemistry & Behavior, 10:149-154.

Gerlach, M., Riederer, P., Przuntek, H., Youdim, M. B. H., (1991) MPTP mechanisms of neorotoxicity and their implications for Parkinson's disease. European Journal of Pharmacology-Molecular Pharmacology Section, 208:273-286.

Handa, R. J., Roselli, C. E., Horton, L., Resko, J. A., (1987) The quantitative distribution of cytosolic androgen receptors in microdissected areas of the male rat brain: effects of estrogen treatment. Endocrinology, 121:233-240.

Heikkila, R. E., Nicklas, W. J., Vyas, I., Duvoisin, R. C., (1985) Dopaminergic toxicity of rotenone and the 1-methyl-4-phenylpyridinium ion after stereotaxic administration to rats: implication for the mechanism of 1-methyl-4-phenyl-1,2,3,6-tetrahydropyridine toxicity. Neuroscience Letters, 62:389.

Hruska, R. E., (1986) Elevation of striatal dopamine receptors by estrogen: dose and time studies. Journal of Neurochemistry, 47:1905-1915.

Hruska, R. E., Ludmer, L. M., Pitman, K. T., De Ryck, M., Silberberg, E. K., (1982) Effects of estrogen on striatal dopamine receptor function in male and female rats. Pharmacol. Biochem. Behav., 16:285-291.

Hruska, R. E., Silbergeld, E. K., (1980) Estrogen treatment enhances dopamine receptor sensitivity in the rat. Eur. J. Pharmacol., 61:397-400.

Irwin, I., Langston, J. W., (1985) Selective accumulation of MPP^+ in the substantia nigra: a key to neurotoxicity ? Life Sciences, 36:207-212.

Javitch, J. A., Uhl, G. R., Snyder, S. H., (1984) Parkinsonism-inducing neurotoxin, N-methyl-4-phenyl-1,2,3,6-tetrahydropyridine: characterization and localization of receptor binding sites in rat and human brain. Proc. Natl. Acad. Sci., USA, 81:4591-4595.

Javitch, J. A., D'Amato, R. J., Strittmatter, S. M., Snyder, S. H., (1985) Parkinsonism-inducing neorotoxin, N-methyl-4-phenyl-1,2,3,6-tetrahydropyridine: uptake of the matabolite N-methyl-4-phenylpyridine by dopamine neurons explains selective toxicity. Proc. Natl. Acad. Sci., 82:2173-2177.

Jellinger, K., Pathology of Parkinson's Syndrome. In: Calne, D. B., ed. Handbook of Experimental Pharmacology, Vol. 88, Springer, Berlin-Heidelberg, 1989, p. 47.

Kandel, E. R., Schwartz, J. H., Jessel T.M., Principles of Neural Science, 3rd Ed., New York: Elsevier Science Publishing Co., Inc., 1991, pp. 151; 523-535; 655;863.

Kizer, J. S., Humm, J., Nicholson, G., Greeley, G., Youngblood, W., (1978) The effect of castration, thyroidectomy and haloperidol upon the turnover rates of dopamine and norepinephrine and the kinetic properties of tyrosine hydroxylase in discrete hypothalamic nuclei of the pale rat. Brain Research, 146:95-107.

Lehninger, A. L., Nelson, D. L., Cox, M. M., Principles of Biochemistry. 2nd Ed., New York: Worth Publishers, Inc., 1993, pp. 713-714.

Le'vesque, D., Di Paolo, T., (1988) Rapid conversion of high into low striatal D2-dopamine receptor agonist binding states after an acute physiological dose of 17 beta-estradiol. Neuroscience Letters, 88:113-118.

Maidment, N. T., Martin, K. F., Ford, A. P. D., Marsden, C. A., In Vivo Voltammetry: The Use of Carbon-Fiber Electrodes to Monitor Amines and Their Metabolites. In: Boulton, A. A., Baker, G. B., Vanderwolf, C. H., eds. Neuromethods, Vol. 14: Neurophysiological Techniques: Basic Methods and Concepts. NJ: The Humana Press, Inc., 1990; 321-383.

McDermott, J. L., Liu, B., Dluzen, D. E., (1994) Sex differences and effects of estrogen on dopamine and DOPAC release from the striatum of male and female CD-1 mice. Experimental Neurology, 125:306-311.

Mitchell, J. B., Stewart, J., (1989) Effects of castration, steroid replacement, and sexual experience on mesolimbic dopamine and sexual behavior in the male rat. Brain Research, 491:116-127.

Mizuno, Y., Sone, N., Saitoh, T., (1987) Effects of 1-methyl-4-phenyl-1,2,3,6-tetrahydropyridine and 1-methyl-4-phenylpyridinium ion on activities of the enzymes in the electron transport system in mouse brain. Journal of Neurochemistry, 48:1787.

Nicklas, W. J., Vyas, I., Heikkila, R. E., (1985) Inhibition of NADH-linked oxidation in brain mitochondria by 1-methyl-4-phenylpyridine, a metabolite of the neurotoxin, 1-methyl-4-phenyl-1,2,3,6-tetrahydropyridine. Life Sci., 36:2503.

Pahwa, R., Koller, W. C., Defining Parkinson's Disease and Parkinsonism. In: Ellenberg, J. H., Koller, W. C., Langston, J. W., eds. Etiology of Parkinson's Disease. New York: Marcel Dekker, Inc., 1995; 1-4.

Palacios, J. M., Wiederhold, K. H., (1984) Acute administration of 1-N-methyl-4-phenyl-1,2,3,6-tetrahydropyridine (MPTP), a compound producing parkinsonism in humans, stimulates [2-^{14}C] deoxyglucose uptake in the region of the catecholaminergic cell bodies in the rat and guinea pig brains. Brain Research, 301:187-191.

Paxinos, G., Watson, C., The Rat Brain In Stereotaxic Coordinates, 4th Ed., Academic Press, a division of Harcourt Brace & Company, San Diego, CA, 1998.

Pellegrino, L. J., Pellegrino, A. S., Cushman, A. J., A Stereotaxic Atlas of the Rat Brain. 2nd Ed. New York: Plenum Press, 1979; pp. 22-23.

Poirier, J., Donaldson, J., Barbeau, A., (1985) The specific vulnerability of the substantia nigra to MPTP is related to the presence of transition metals. Biochemical and Biophysical Research Communications, 128:25-33.

Ramirez, V. D., Zheng, J., Siddique, K. M., (1996) Membrane receptors for estrogen, progesterone, and testosterone in the rat brain: fantasy or reality. Cellular and Molecular Neurobiology, 16:175-198.

Ramsay, R. R., Salach, J. I., Dadgar, J., Singer, T. P., (1986) Inhibition of mitochondrial NADH dehydrogenase by pyridine derivatives and its possible relation to experimental and idiopathic parkinsonism. Biochem. Biophys. Res. Commun, 135:269.

Ransom, B. R., Kunis, D. M., Irwin, I., Langston, J. W., (1987) Astrocytes convert the parkinsonism inducing neurotoxin, MPTP, to active metabolite, MPP^+. Neuroscience Letters, 75:323-328.

Scherman, D., Darchen, F., Desnos, C., Henry, J. P., (1988) 1-Methyl-4-phenylpyridinium is a substrate of the vesicular monoamine uptake system of chromaffin granules. European Journal of Pharmacology, 146:359-360.

Schumacher, M., (1990) Rapid membrane effects of steroid hormones: an emerging concept in neuroendocrinology. TINS, 13:359-362.

Scotcher, K. P., Irwin, I., DeLanney, L. E., Langston, J. W., DiMonte, D., (1990) Effects of 1-methyl-4-phenyl-1,2,3,6-tetrahydropyridine and 1-methyl-4-phenylpyridinium ion on ATP levels of mouse brain synaptosomes. Journal of Neurochemistry, 54:1295.

Session, D. R., Pearlstone, M. M., Jewelewicz, R., Kelly, A. C., (1994) Estrogens and Parkinson's Disease. Medical Hypotheses, 42:280-282.

Singer, T. P., Castagnoli, Jr., N., Ramsay, R. R., Trevor, A. J., (1987) Biochemical events in the development of parkinsonism induced by 1-methyl-4-phenyl-1,2,3,6-tetrahydropyridine. Journal of Neurochemistry, 49:1.

Smith, A. D., Bolam, J. P., (1990) The neural network of the basal ganglia as revealed by the study of synaptic connections of identified neurons. TINS, 13:259-265.

Steranka, L. R., Polite, L. N., Perry, K. W., Fuller, R. W., (1983) Dopamine depletion in rat brain by MPTP (1-methyl-4-phenyl-1,2,3,6-tetrahydropyridine). Res. Commun. Sub. Abuse, 4:315-319.

Thompson, R. F., The Brain: An Introduction to Neuroscience. New York: W.H. Freeman and Company, 1985.

Vyas, I., Heikkila, R. E., Nicklas, W. J., (1986) Studies on the neurotoxicity of 1-methyl-4-phenyl-1,2,3,6-tetrahydropyridine: inhibition of NAD-linked substrate oxidation by its metabolite, 1-methyl-4-phenylpyridinium. Journal of Neurochemistry, 46:1501.

Yamada, Y., Nishida, E., (1978) Effects of estrogen and adrenal androgen on unit activity of the rat brain. Brain Research, 142:187-190.